Follow-up analyses of the BNS signals GW170817 and GW190425 by using PN waveform models

Tatsuya Narikawa, Nami Uchikata
(ICRR, The University of Tokyo)

ICRR Institute for Cosmic Ray Research University of Tokyo

arXiv:2205.06023

LIGO G2200305 JGW-G2214036

LIGO VIRGO KAGRA

Contents

(1) Science targets of data analyzing BNS-GWs

(2) Brief review on BNS data analyses

(3) Follow-up analyses of GW170817 with PNTidal

arXiv:2205.06023

(1) Science targets of data analyzing BNS-GWs

BNS coalescences are valuable laboratories for nuclear astrophysics

Schematic phase diagram for dense nuclear matter

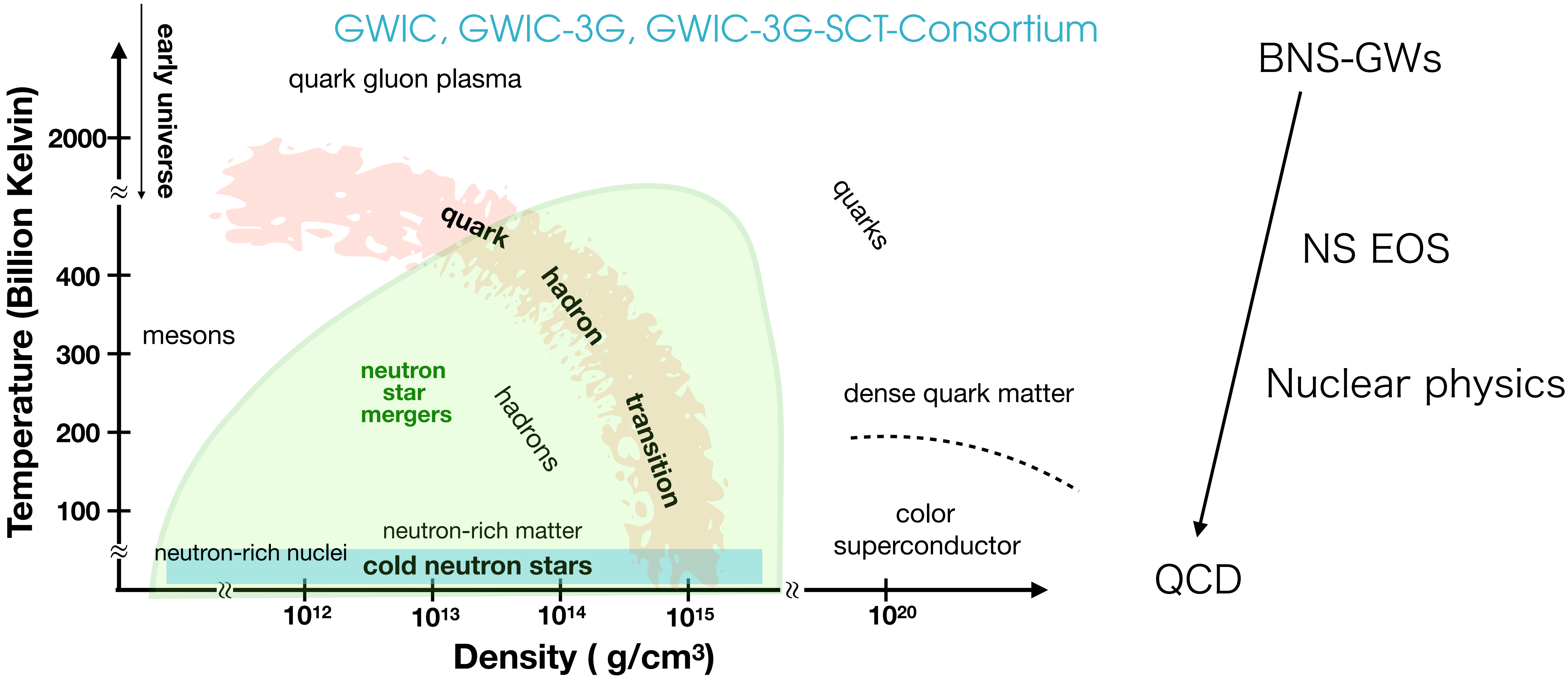

BNS-GWs can provide complementary information on the macroscopic properties of neutron stars and the dense matter.

Review [Lattimer&Prakash2016; Baiotti2019; Dietrich, Hinderer, Samajdar 2021; Chatziioannou2020]

Tidal deformability λ

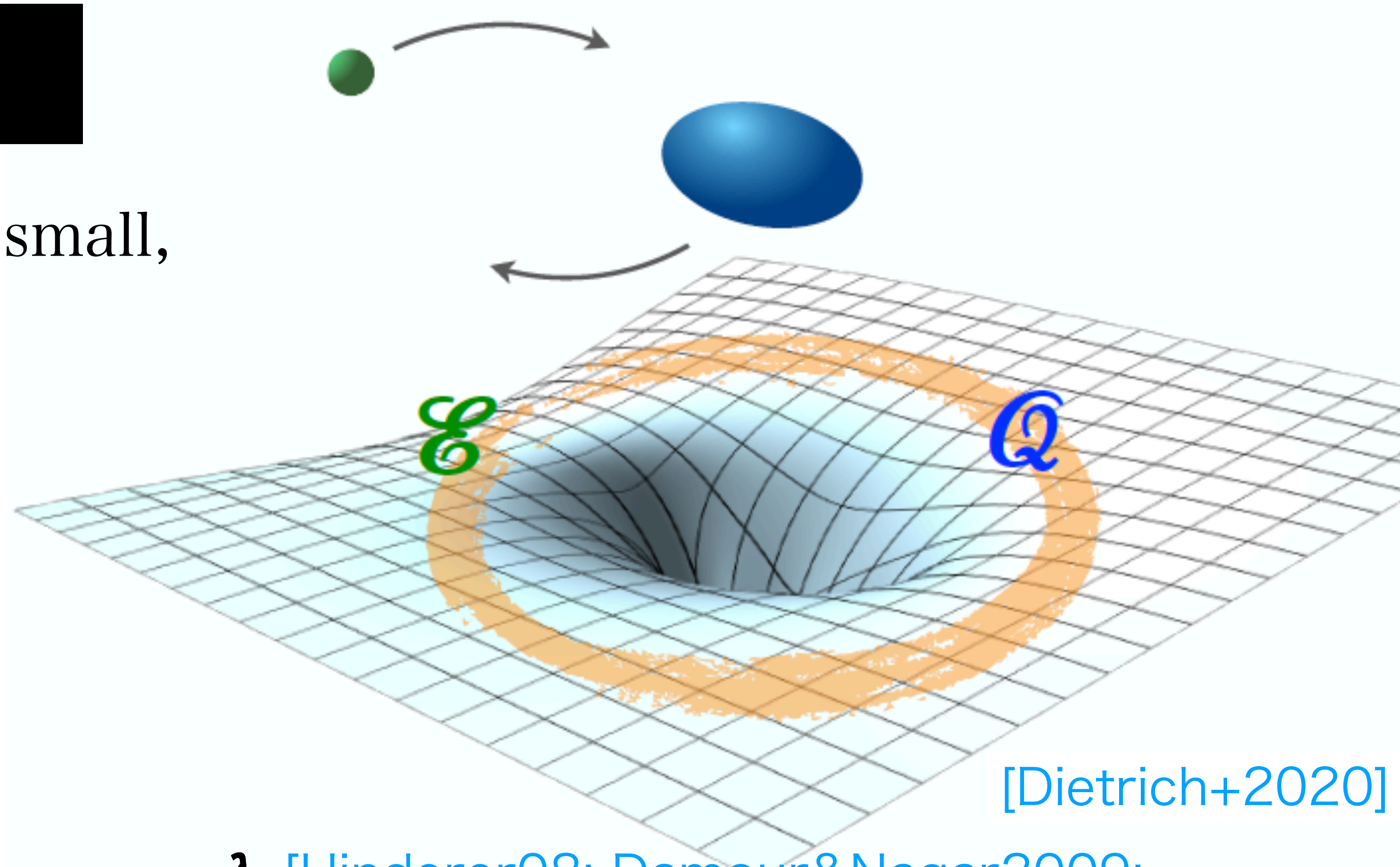

When binary orbital separations are small, each star is tidally distorted by its companion.

$$\lambda := -\frac{Q_{ij}}{E_{ij}}$$

Q_{ij}: tidally induced quadrupole moment

E_{ij}: companion's tidal field

$\boldsymbol{\lambda}$ [Hinderer08; Damour&Nagar2009; Postnikov+2010]

The tidal deformability of NS matter affects the GW signals and characterizes NS EOS models.

Binary tidal deformability $\tilde{\Lambda} = \frac{16}{13}\left[(1+11X_2)X_1^4\Lambda_1 + (1 \leftrightarrow 2)\right]$

$\Lambda_{1,2} = \lambda_{1,2}/m_{1,2}^5$: individual ones $\quad X_{1,2} = m_{1,2}/(m_1+m_2)$: mass ratio

PNTidal [Flanagan&Hinderer08; Damour, Nagar, Villain 2012; Henry, Faye, Blanchet 2020; Narikawa, Uchikata, Tanaka 2021]

PN waveform phase modeling has advanced in recent years.

$\chi_{\rm eff}$: spin
Difficult to measure well

for TF2_PNTidal

η: symmetric mass ratio
Difficult to measure well

$$\Psi_{\rm BNS}(f) = \Psi_{\rm BBH}(f) + \Psi_{\rm Tidal}(f)$$

$$\sim \mathcal{M}^{-5/3} f^{-5/3} \left[1 + a_{\rm 1PN}(\eta) x^2 + a_{\rm 1.5PN}(\eta, \chi_{\rm eff}) x^3 \right.$$

$\mathcal{M}$:chirp mass
Measurable very well

$$\left. + a_{\rm 2PN}(\eta, \chi_i^2, \kappa_s) x^4 + \ldots + a_{\rm 5PN}(\tilde{\Lambda}) x^{10} + \ldots \right]$$

v: orbital velocity

$$x = (\pi M f)^{2/3} = v^2$$

κ: spin-induced QM
NS EOSs

Λ: tidal deformability
NS EOSs

Post-Newtonian (PN) theory is theoretically rigid and can efficiently describe the inspiral regime.

Sophisticated models: EOB, IMRPhenom and NR calibrated models are constructed by extension of the PN theory.

PN formalism review [Blanchet2014; Poisson&Will2014; Isoyama, Nakano, Sturani 2020]
TF2 (3.5PN) [Dhurandhar+1994; Buonanno+2009] **Spin** summarized in [Khan+2016]
PNTidal [Flanagan&Hinderer08; Damour, Nagar, Villain 2012; Henry+2020; Narikawa+2021]

GW inference on GW170817 [LVC 2017, 2018]

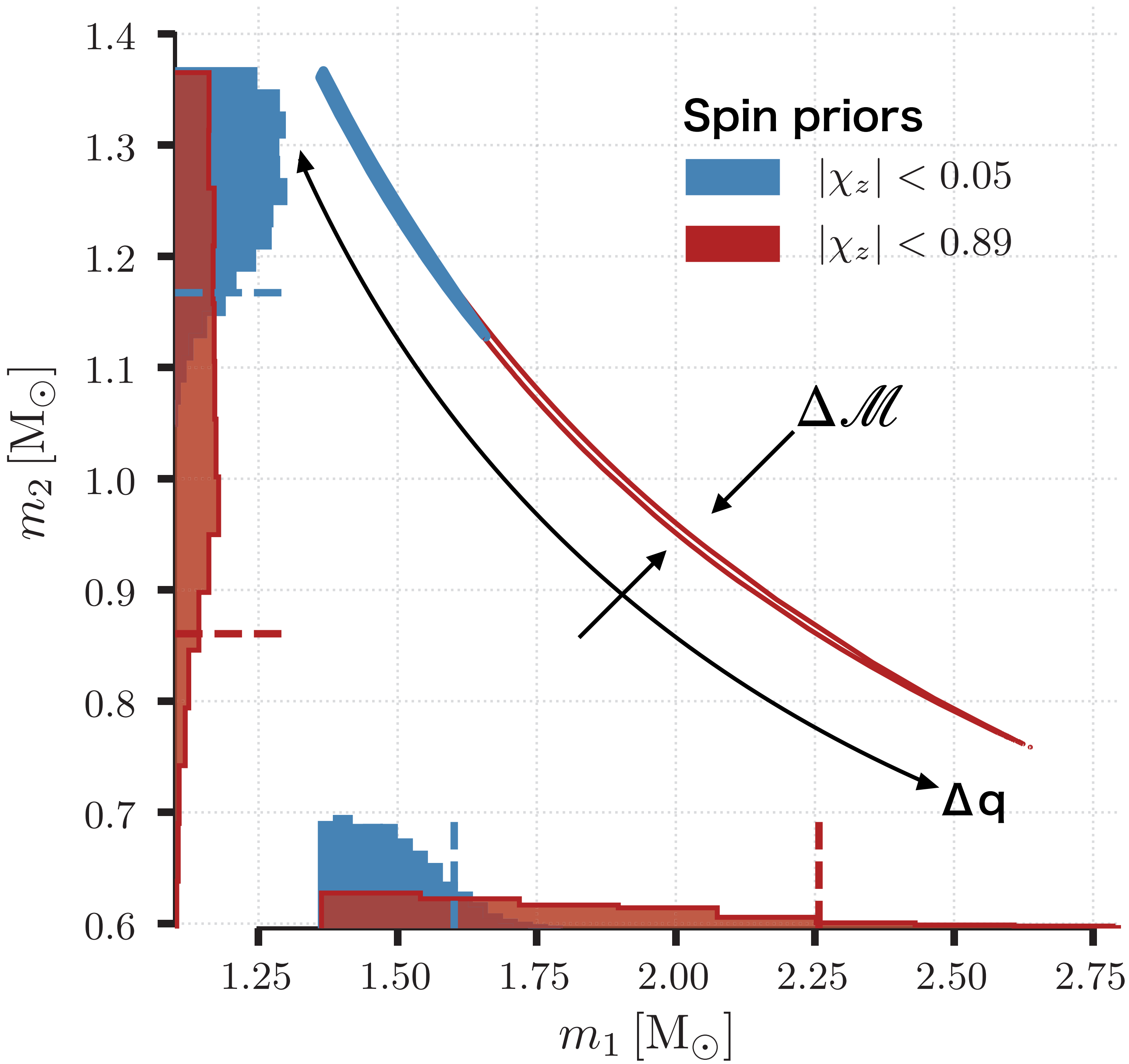

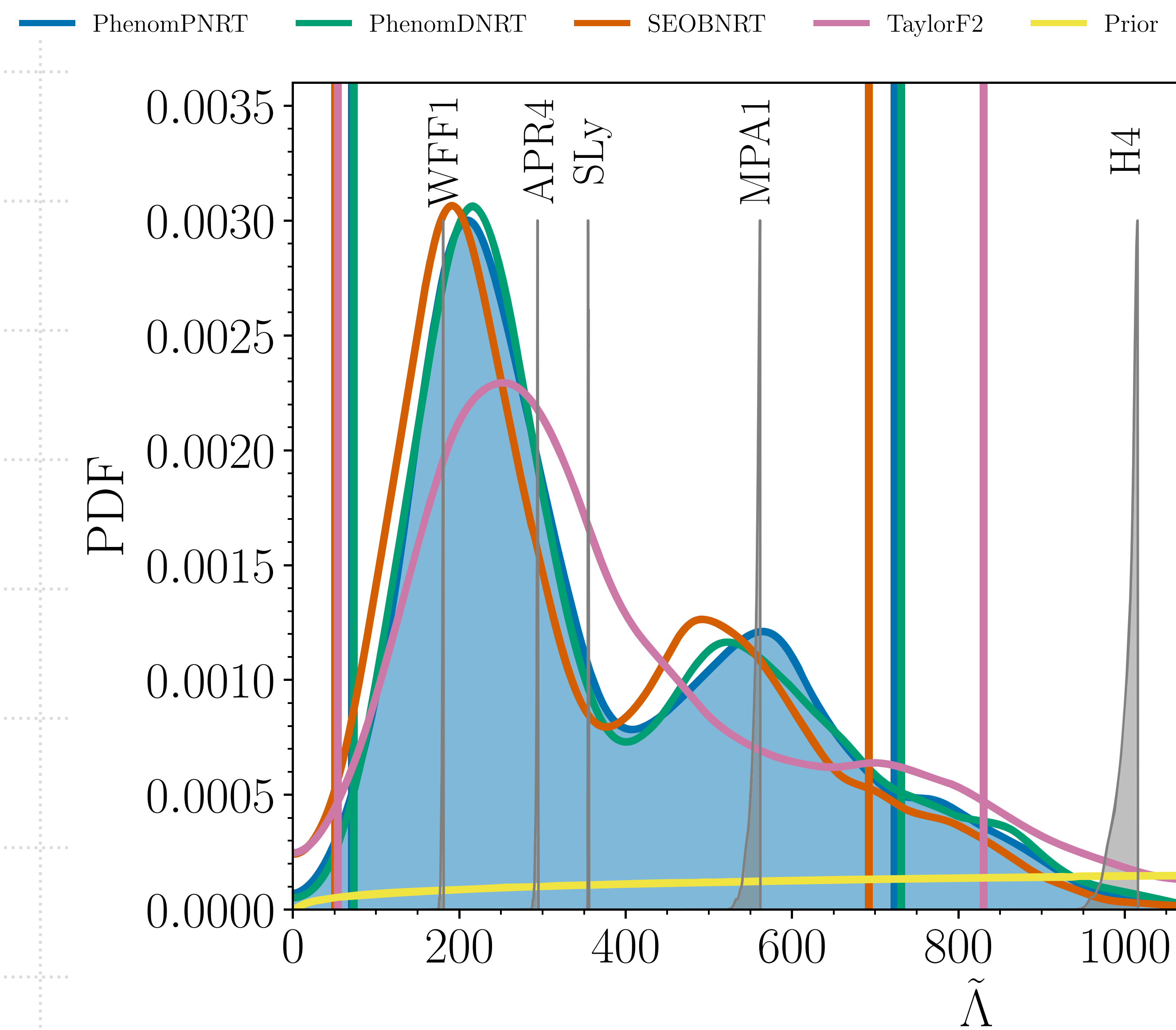

$\mathscr{M}$: measured well. q: not measured well.
q-$\chi_{\rm eff}$ correlation

$\tilde{\Lambda}$: measured, less compact EOS models are disfavored.

[De+2018; Dai+2018; LVC2019; Narikawa+2018,2019; Chatziioannou2020]

NRTidal [Dietrich+2017]

Current estimated BNS merger rate $320^{+490}_{-240}\ \mathrm{Gpc^{-3}yr^{-1}}$ [LVC 2021]

Projected EOS constraints from expected BNS coalescences

In O4 and O5, statistical uncertainty in radius $\Delta R \sim \mathcal{O}(1)$ km. [Landry+2020]

Statistical uncertainty

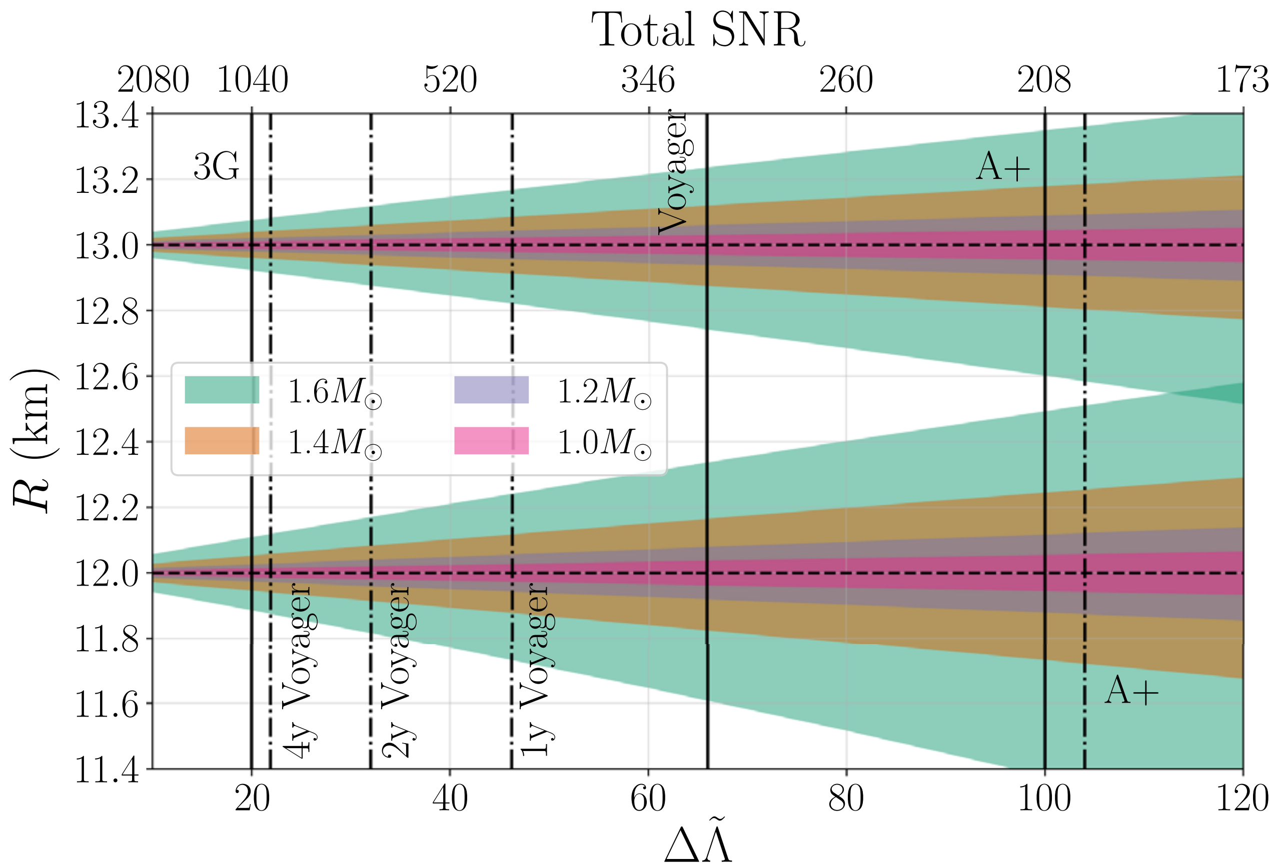

Required waveform phase uncertainty

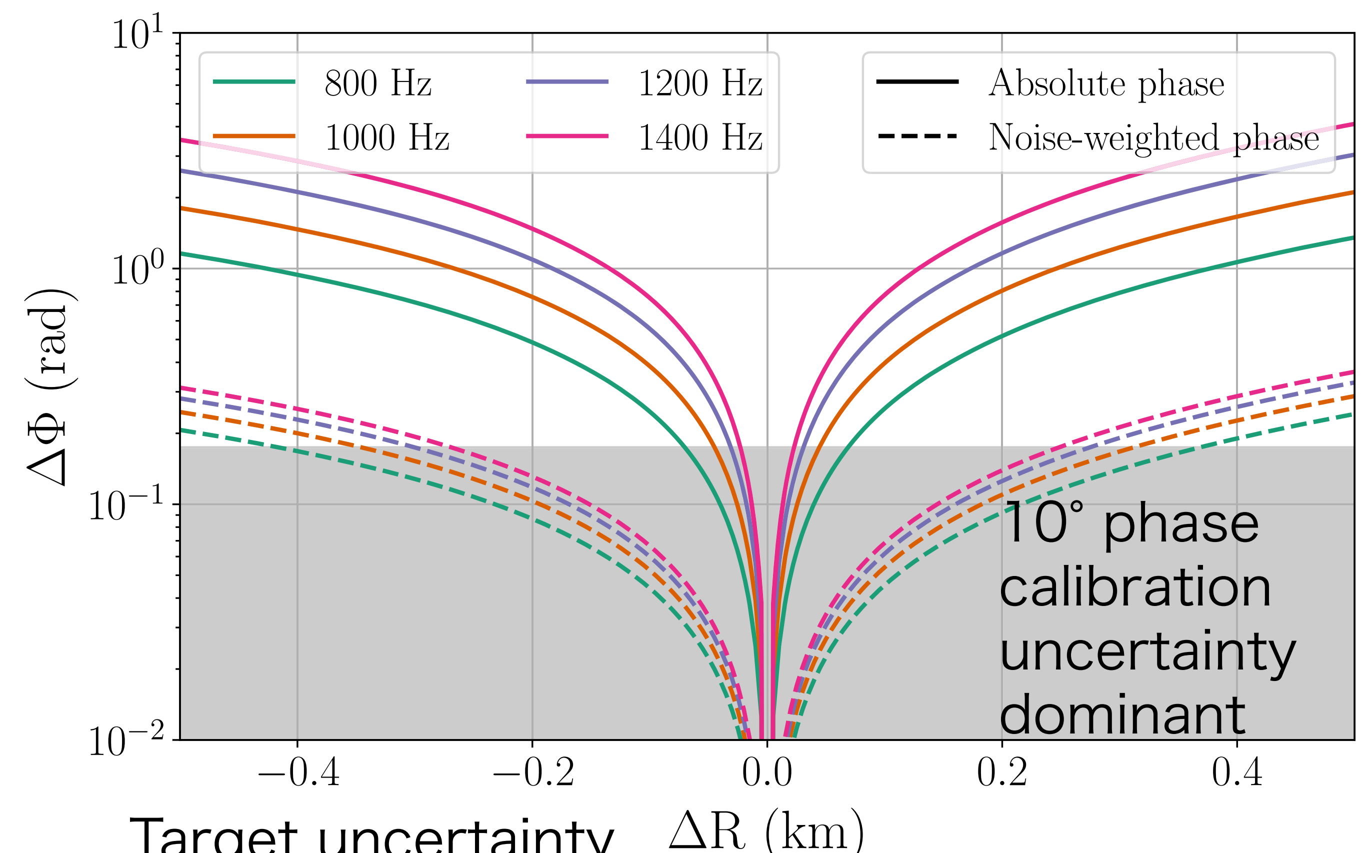

For A+, $\Delta\tilde{\Lambda} \sim 100$ and $\Delta R \sim 500$ m.
For 3G, $\Delta\tilde{\Lambda} \sim 20$ and $\Delta R \sim 100$ m.
(For GW170817, $\Delta\tilde{\Lambda} \sim 650$ at SNR 32)

$\Delta R \sim 500$ m —> 3-4 rad dephasing.
$\Delta R \sim 100$ m —> 0.5-1 rad dephasing.

[Chatziioannou 2022]

→ Further improve waveform model to avoid bias.

(2) Review on BNS data analyses

① BNS signal injection studies

[Dudi+2018; Samajdar&Dietrich2018,2019; Messina+2019; Agathos+2020; Gamba+, 2021; Kunert+2021]

② GW170817 analyses: Waveform systematics

[LVC2019; Narikawa+2019; Gamba+, 2021; Ashton&Dietrich2021]

③ GW170817 analyses: Waveform model comparison

[Gamba+, 2021; Ashton&Dietrich2021]

④ GW170817 analyses: Constraints on NS EOSs

[LVC2017, 2018a, 2018b, 2019; Landry+2018, 2020; Capano+2019; Narikawa+2019]

Review ① BNS signal injection studies

EOB-NR hybrid waveform injections

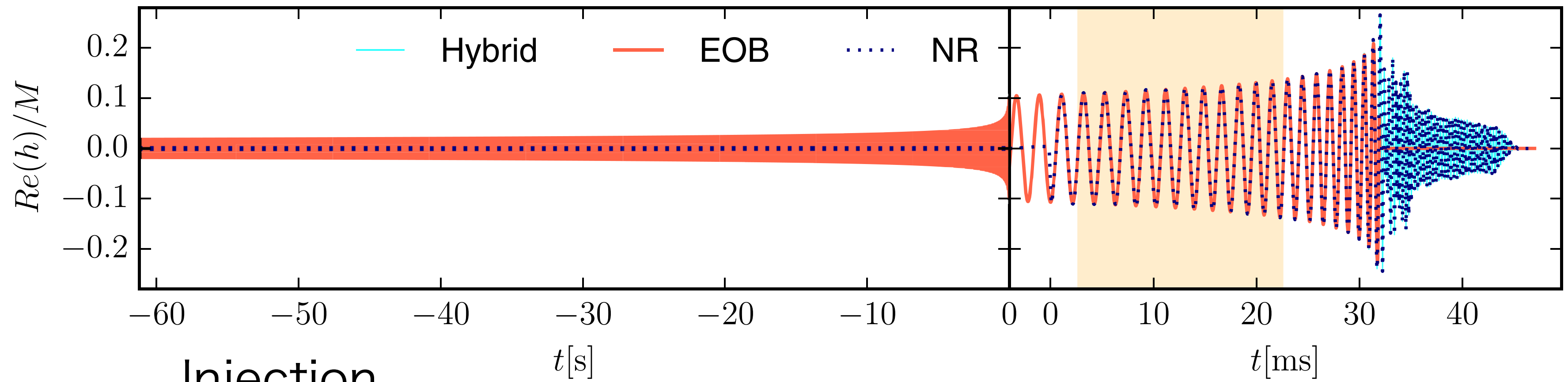

Recovered posteriors

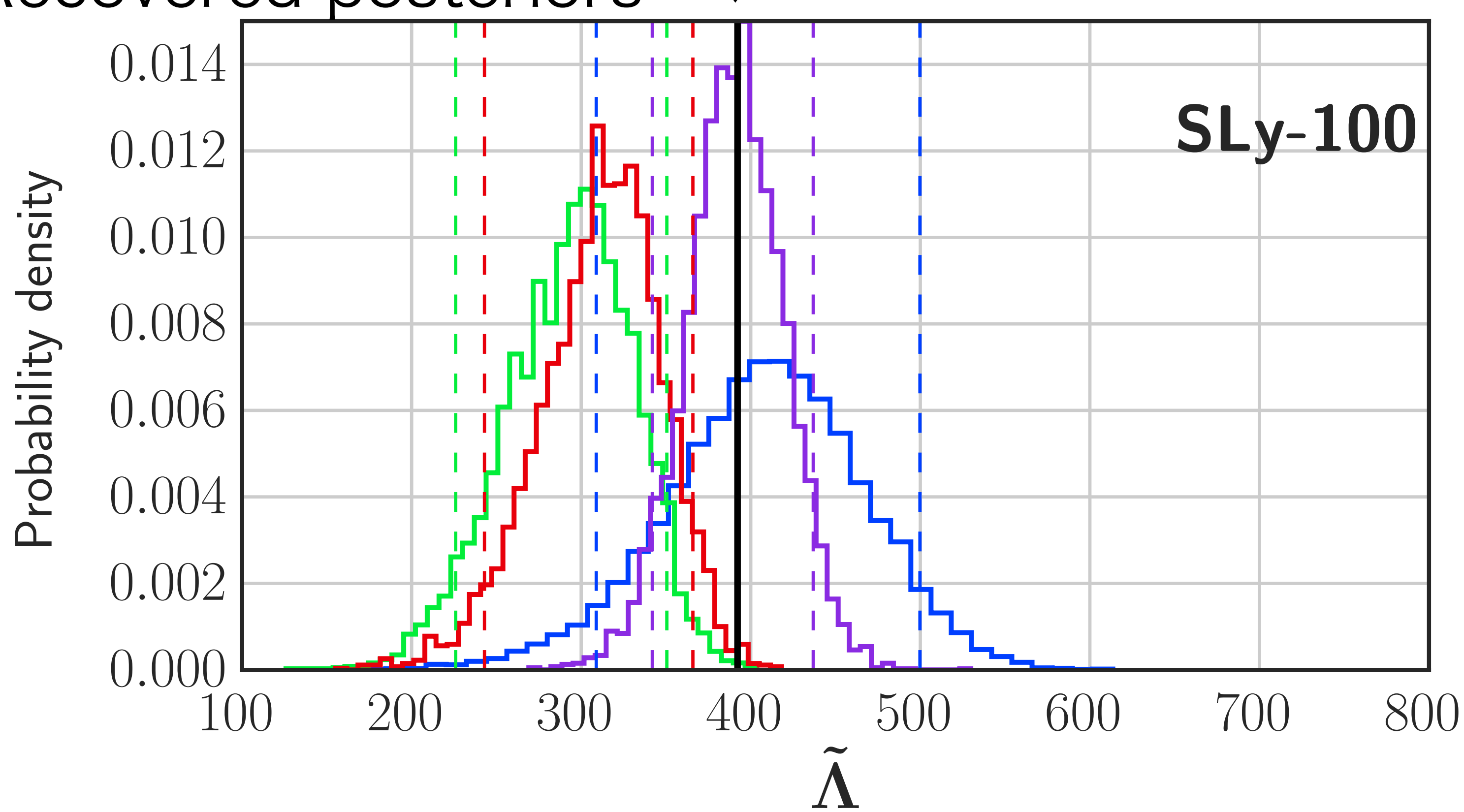

no actual noise is added to the data

SNR=100

[Dudi+, 2018]

- $\text{TaylorF2}_{\text{Tides}}$
- SEOBNRv4_ROM_NRTidal
- IMRPhenomD_NRTidal
- TEOBResum_ROM

TEOBResumS [Nagar+2018]

An increase of SNR (~100) yields biases in the estimates of $\tilde{\Lambda}$.

Tendency: NRTidal underestimate $\tilde{\Lambda}$. TEOBResumS gives the best estimate.

TaylorF2_PNTidal is broadly consistent with the injected $\tilde{\Lambda}$.

[Dudi+2018; Samajdar&Dietrich2018,2019; Messina+2019; Agathos+2020; Gamba+2021; Kunert+2021]

Review ② GW170817 analyses: Waveform systematics in $\tilde{\Lambda}$

Reanalyses with f_{high}=1024 Hz focusing on inspiral regime

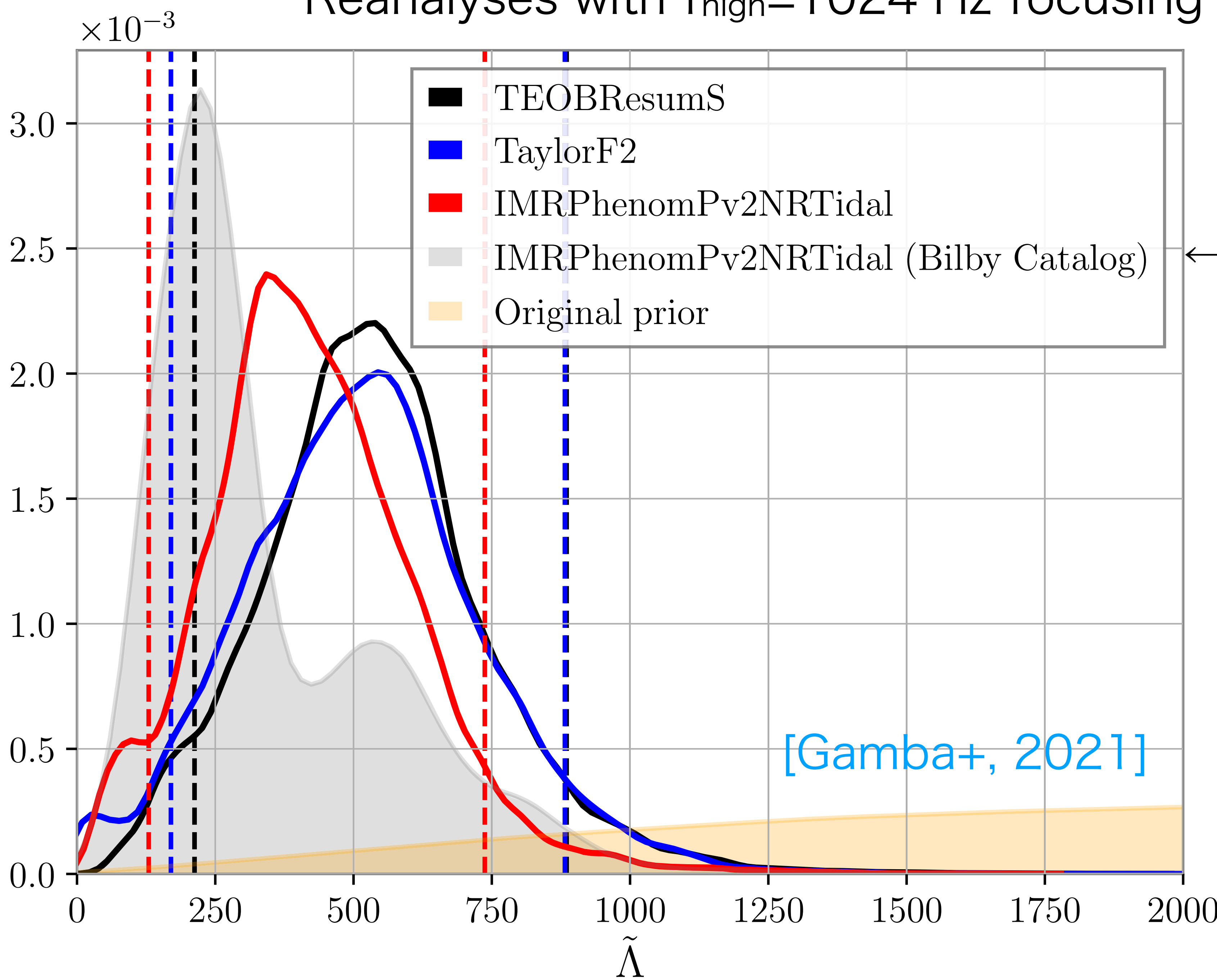

← (f_{high}=2048 Hz) in [LVC 2018]

Inspiral-only analyses, with f_{high}=1024 Hz, give larger and less tighter $\tilde{\Lambda}$ than the IMR analyses, with f_{high}=2048 Hz.
[Dai+2018; Narikawa+19]

NRTidal gives smaller estimates of $\tilde{\Lambda}$ for GW170817 than **TEOBResumS** and **TaylorF2_PNTidal**.

[LVC2019; Narikawa+2019; Gamba+2021; Ashton&Dietrich2021]

Review ③ GW170817 analyses: Waveform model comparison with a “hypermodel” approach

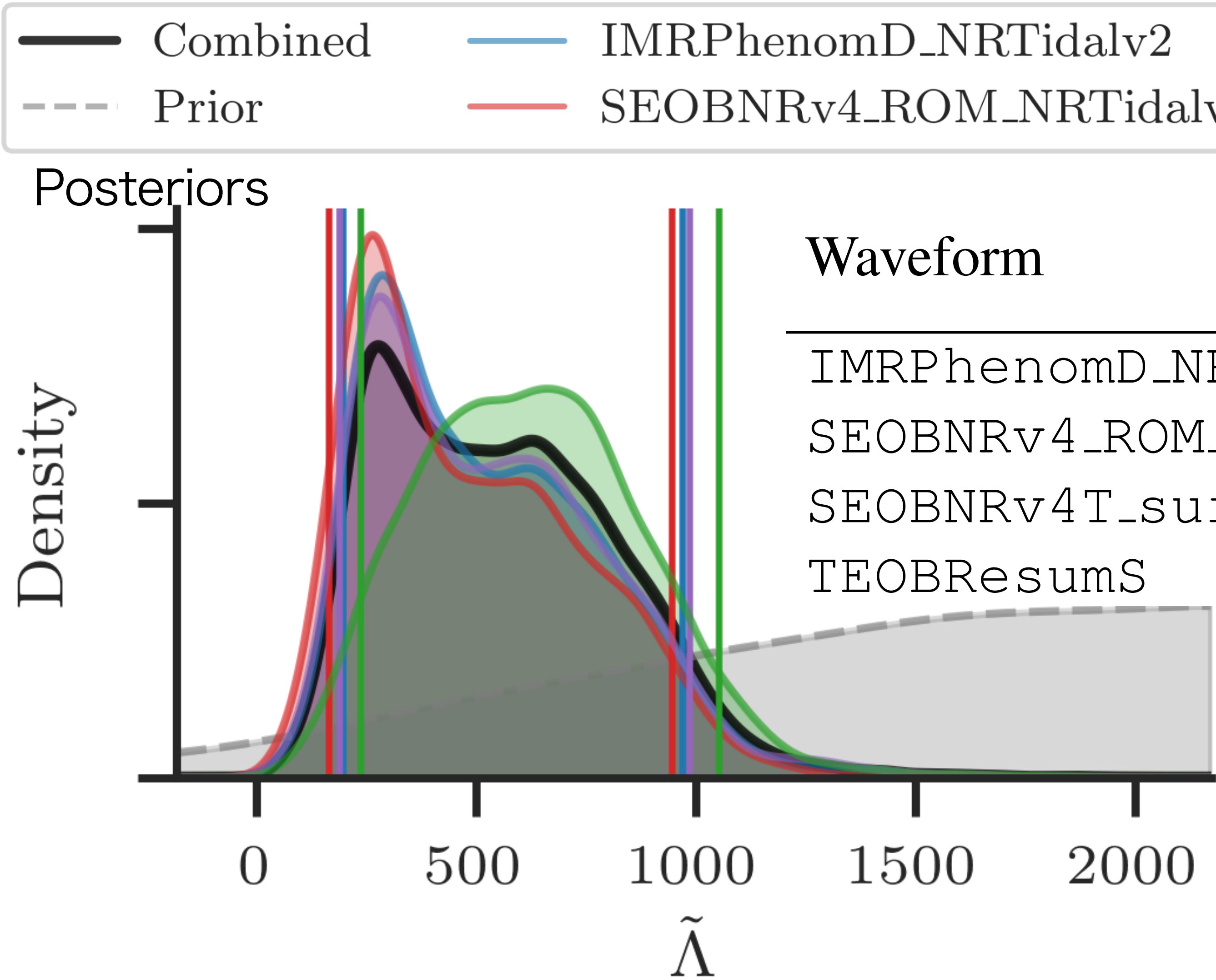

Waveform	GW170817		
	Prob. [%]	Odds	
IMRPhenomD_NRTidalv2	23.2 ± 0.6	1.40 ± 0.04	(1.6 ± 0.3)
SEOBNRv4_ROM_NRTidalv2	20.5 ± 0.6	1.59 ± 0.05	(1.9 ± 0.4)
SEOBNRv4T_surrogate	23.8 ± 0.6	1.37 ± 0.04	(1.4 ± 0.3)
TEOBResumS	32.5 ± 0.6	—	

hypermodels

(Nested sampling)

[Ashton & Dietrich 2021]

TEOBResumS is the most successful at predicting GW170817 data.

Although the odds do not exceed the threshold of a significant preference to TEOBResumS, they stress that the mild preference to TEOBResumS over NRTidalv2 and SEOBNRv4T is worthy of further investigation.

(See [Gamba+, 2021] for model comparison.)

NRTidalv2 [Dietrich+2018]

Review ④ GW170817 analyses: Constraints on NS EOSs

[LVC 2018]

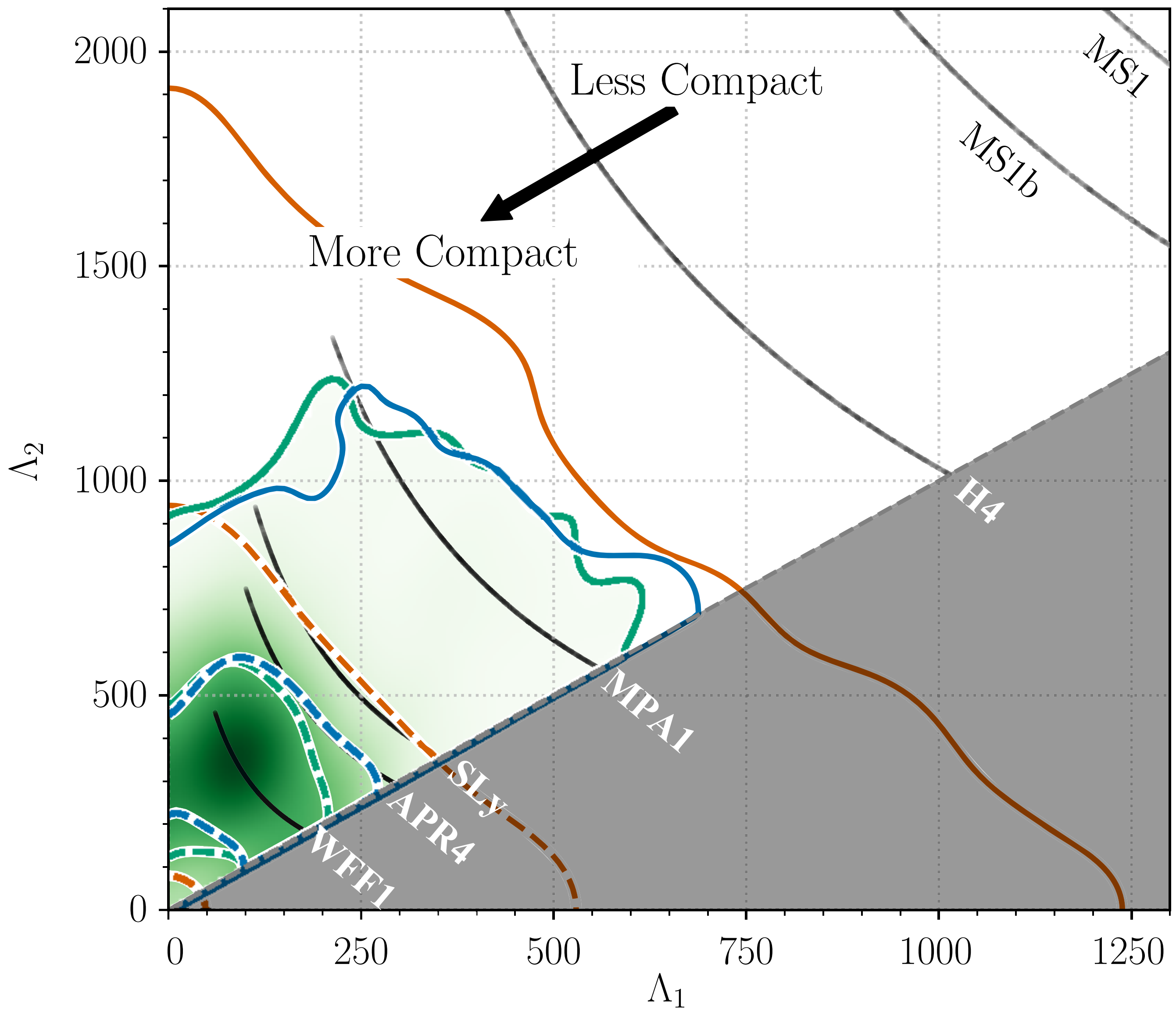

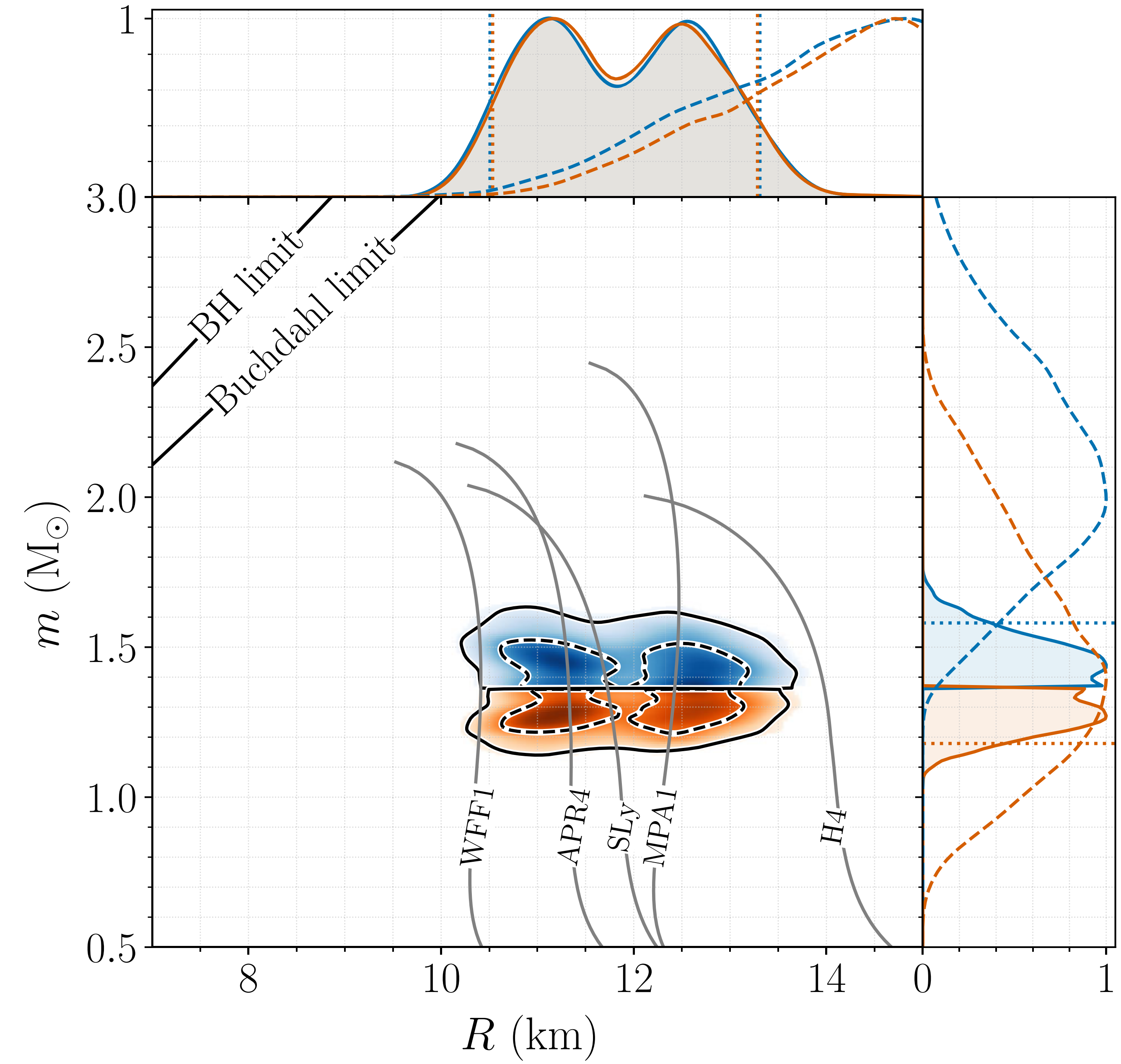

Independent EOSs
EOS-insensitive universal relations
Spectral EOS parametrization

$$R_1 = 11.9^{+1.4}_{-1.4}\ \mathrm{km} \quad R_2 = 11.9^{+1.4}_{-1.4}\ \mathrm{km}$$

$\boxed{\text{Less compact EOS models are disfavored.}}$

[LVC2017, 2018a, 2018b, 2019; Landry+2018, 2020; Capano+2019; Narikawa+2019]

What we learn:

・Injection study tendency: **NRTidal** underestimate $\tilde{\Lambda}$. **TEOBResumS** gives the best estimate. **TF2_PNTidal** is broadly consistent with the injected $\tilde{\Lambda}$.

・GW170817 analyses: **NRTidal** might bias $\tilde{\Lambda}$ smaller.

Motivated by these, we will do the following.

(3) Follow-up analyses of GW170817 and GW190425 with PNTidal focusing on the inspiral regime (f_{high}=1000 Hz).

arXiv:2205.06023

Waveform systematics & Waveform model comparison:

❶ Comparison among point-particle part,

❷ Comparison among different PN orders in PNTidal,

❸ Comparison between PNTidal and NR calibrated models, and

❹ Constraints on NS EOSs

Point-particle phasing

TF2 (up to 3.5PN for phase, 3PN for amplitude)

Extended models:

TF2g (5.5PN for phase) is derived by the Taylor expansion of the EOB formula,

TF2+ (6PN for phase and amplitude) is derived by the fitting to SEOBNRv2

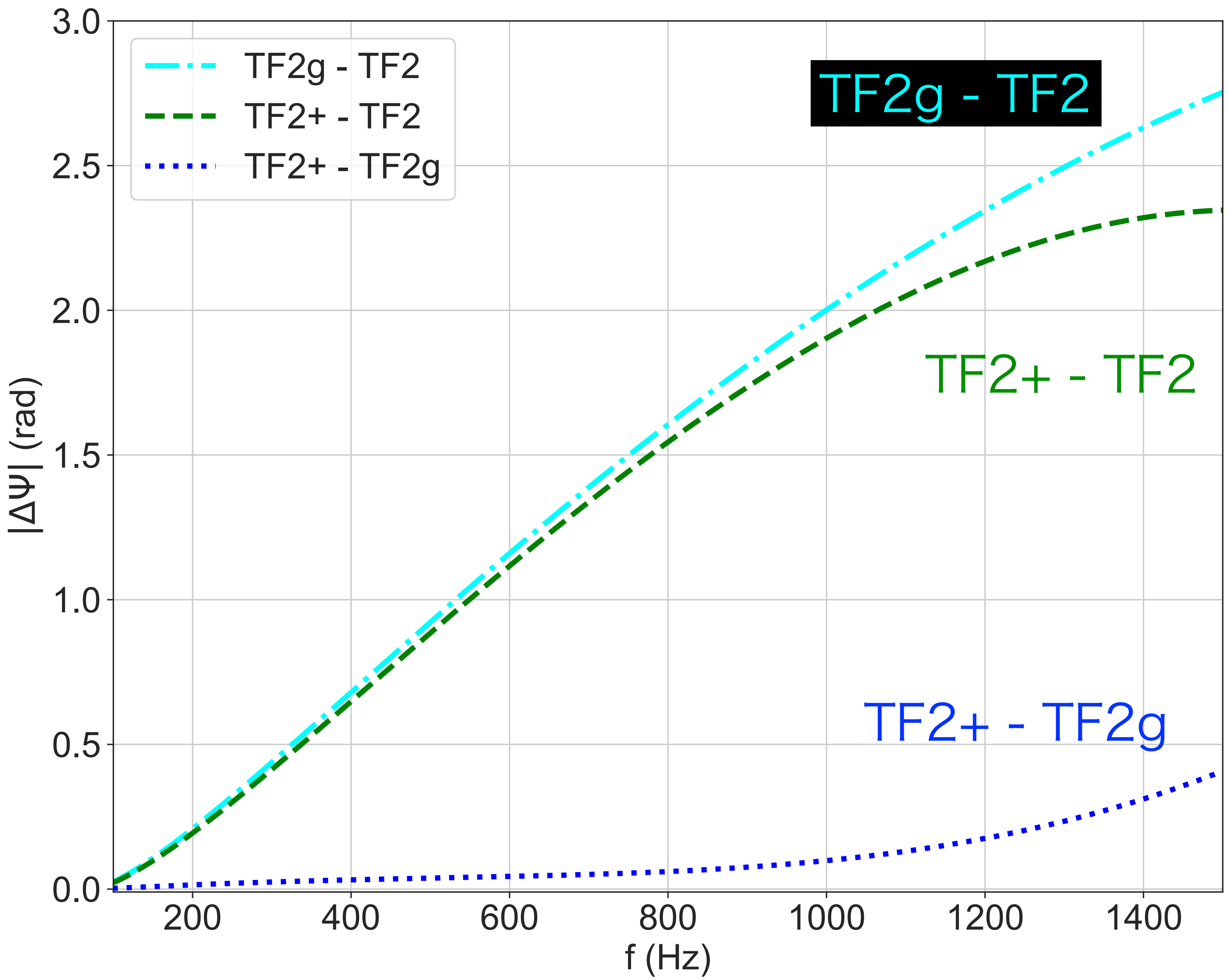

alined for 10 Hz < f < 100 Hz

demonstrated for un-equal mass binary with 1.68+1.13 $M_\odot$

TF2+ - TF2g is less than 0.5 (rad) up to 1500 Hz.

TF2g [Messina+, 2019] TF2+ [Kawaguchi+, 2018]

PN tidal theory

Post-Newtonian (PN) approximation: solve the Einstein eqs. by a series in v/c.
PN theory is theoretically rigid and can efficiently describe the GW emission in the inspiral regime. (valid for slow-motion and weak-field)

PN tidal phase has been derived up to 2.5PN (relative 5+2.5PN) order [Flanagan&Hinderer08; Damour, Nagar, Villain2012]. (**PNTidal**)

Recently, the complete and correct PN tidal phase up to 2.5PN order have been derived
[Henry, Faye, Blanchet 2020; Narikawa, Uchikata, Tanaka 2021].

However, the correct **PNTidal** model has not been used in BNS analyses yet.
In this work, we first use it in BNS analyses.

The old GW tidal phase (incomplete and incorrect)

Agathos et al (2015) [App. B in Damour+2012] $X_A = m_A/(m_A + m_B)$ $\Lambda_A = \lambda_A/m_A^5$

$$\Psi_{\mathrm{Agathos}}(f) = \frac{3}{128\eta}x^{5/2}\sum_{A=1}^{2}\frac{\lambda_A}{M_{\mathrm{tot}}^5 X_A}\Big[-24(12-11X_A) - \frac{5}{28}(3179 - 919X_A - 2286X_A^2 + 260X_A^3)x$$

$$+24\pi(12-11X_A)x^{3/2}$$

incomplete 5+2PN

$$-24\left(\frac{39927845}{508032} - \frac{480043345}{9144576}X_A + \frac{9860575}{127008}X_A^2 - \frac{421821905}{2286144}X_A^3 + \frac{4359700}{35721}X_A^4 - \frac{10578445}{285768}X_A^5\right)x^2$$

$$+\frac{\pi}{28}(27719 - 22127X_A + 7022X_A^2 - 10232X_A^3)x^{5/2}\Big],$$

incorrect 5+2.5PN

The updated complete and corrected GW tidal phase

We rewrote **the complete and corrected form** derived by Henry, Faye, and Blanchet (2020) for the mass quadrupole interactions as a function of the dimensionless tidal deformability $\Lambda_{1,2}$, **in a convenient way for analysis,** by

[Narikawa, Uchikata, Tanaka (2021)]

$$\Psi_{\mathrm{HFB}}(f) = \frac{3}{128\eta}x^{5/2}\sum_{A=1}^{2}\Lambda_A X_A^4\Big[-24(12-11X_A) - \frac{5}{28}(3179 - 919X_A - 2286X_A^2 + 260X_A^3)x$$

$$+24\pi(12-11X_A)x^{3/2}$$

$$-5\left(\frac{193986935}{571536} - \frac{14415613}{381024}X_A - \frac{57859}{378}X_A^2 - \frac{209495}{1512}X_A^3 + \frac{965}{54}X_A^4 - 4X_A^5\right)x^2$$

complete 5+2PN

$$+\frac{\pi}{28}(27719 - 22415X_A + 7598X_A^2 - 10520X_A^3)x^{5/2}\Big],$$

correct 5+2.5PN

—> We have implemented it and used it in BNS analyses.

Tidal phasing

different PN orders, from 5PN through 5+2.5PN, in PNTidal

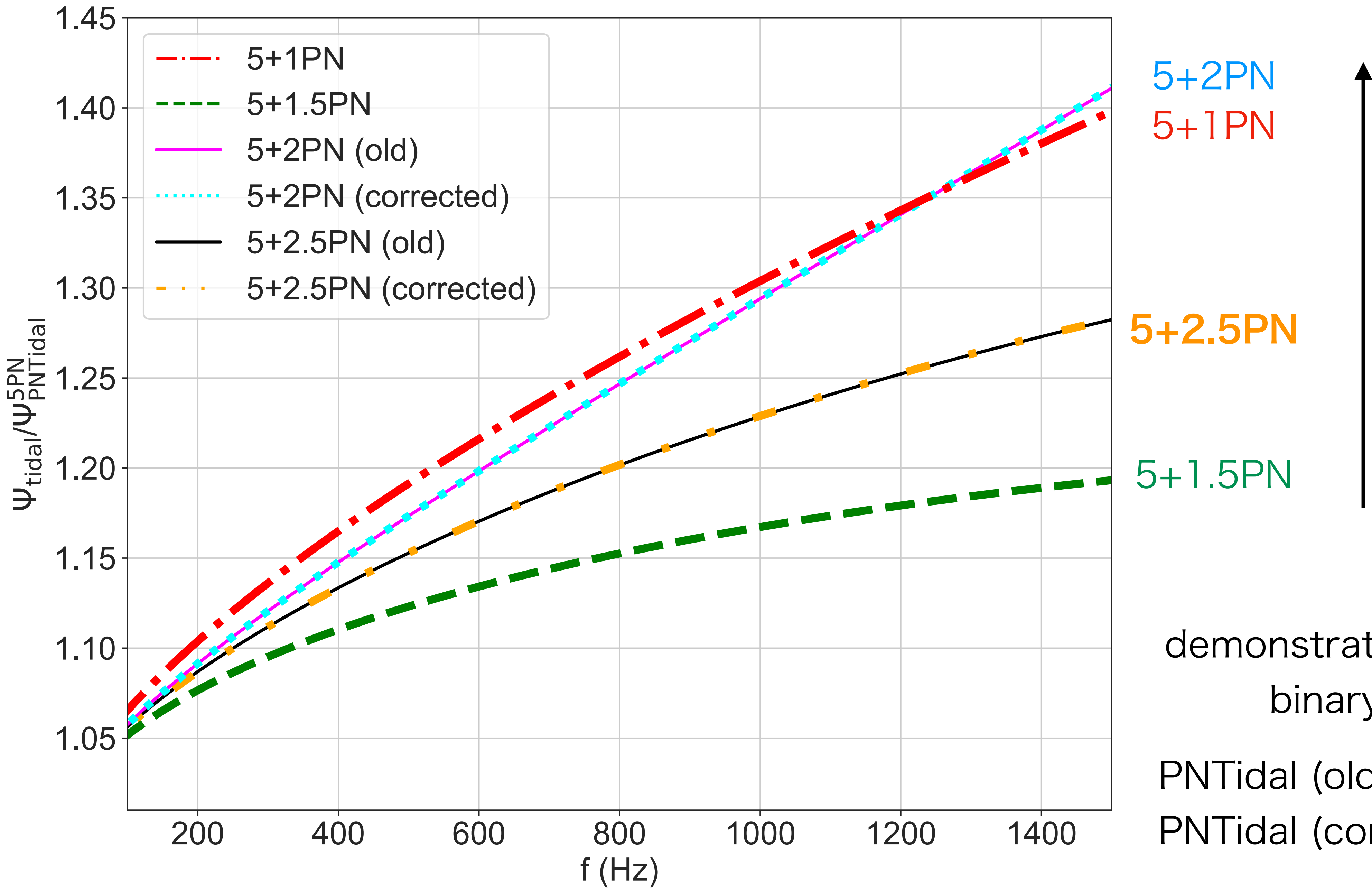

No large difference between the phase shift for **old** and **corrected** PNTidal phase models.

demonstrated for un-equal mass binary, 1.68+1.13 $M_\odot$

PNTidal (old): [Agathos+, 2015].

PNTidal (corrected): [Henry+, 2020].

An increase of PN order does not lead to a monotonic change in the phase shift.

The terms at 5+1PN and 5+2PN give larger phase shift. This is related to the half-PN orders at 5+1.5PN and 5+2.5PN being repulsive.

KyotoTidal

[Kawaguchi+, 2018]

- calibrated by hybrid waveform (**SEOBNRv2T + NR**)
- calibrated only up to 1000 Hz to avoid post-inspiral uncertainties.

Phase employs the PNTidal formula by multiplying the $\tilde{\Lambda}$ by a nonlinear correction

Nonlinear correction

$$\Psi^{\rm KyotoTidal}_{\rm tidal} = \frac{3}{128\eta}\left[-\frac{39}{2}\tilde{\Lambda}\left(1 \boxed{+ a\tilde{\Lambda}^{2/3}x^{p}}\right)\right]x^{5/2}$$

$$\times\left(1+\frac{3115}{1248}x-\pi x^{3/2}+\frac{28024205}{3302208}x^{2}-\frac{4283}{1092}\pi x^{5/2}\right)$$

5PN 5+1PN 5+1.5PN 5+2PN 5+2.5PN

(PNTidal based on Damour+, 2012)

Amplitude is extended by adding the higher-order effects to PNTidal.

$$A_{\rm tidal} = \sqrt{\frac{5\pi\eta}{24}}\frac{m_0^2}{D_{\rm eff}}\tilde{\Lambda}x^{-7/4}$$

$$\times\left(-\frac{27}{16}x^{5}-\frac{449}{64}x^{6}\boxed{-4251\,x^{7.890}}\right).$$

5PN 5+1PN Polynomial function

NRTidal

(NR calibrated)

[Dietrich+, 2017]

another NR calibration approach to describe tidal effects

$$\Psi_{\mathrm{tidal}}^{\mathrm{NRTidal}} = \frac{3}{128\eta}\left[-\frac{39}{2}\tilde{\Lambda}x^{5/2} \times \frac{1+\tilde{n}_1 x+\tilde{n}_{3/2}x^{3/2}+\tilde{n}_2 x^2+\tilde{n}_{5/2}x^{5/2}}{1+\tilde{d}_1 x+\tilde{d}_{3/2}x^{3/2}}\right]$$

Pade approximation

NRTidalv2

(NR calibrated)

[Dietrich+, 2019]

NRTidal's update, introduce amplitude

$$\Psi_{\mathrm{tidal}}^{\mathrm{NRTidalv2}} = \frac{3}{128\eta}\left[-\frac{39}{2}\tilde{\Lambda}x^{5/2} \times \frac{1+\tilde{n}'_1 x+\tilde{n}'_{3/2}x^{3/2}+\tilde{n}'_2 x^2+\tilde{n}'_{5/2}x^{5/2}+\tilde{n}'_3 x^3}{1+\tilde{d}'_1 x+\tilde{d}'_{3/2}x^{3/2}+\tilde{d}'_2 x^2}\right]$$

Pade approximation

$$A_{\mathrm{tidal}}^{\mathrm{NRTidalv2}} = \sqrt{\frac{5\pi\eta}{24}}\frac{M_{\mathrm{tot}}^2}{d_L}\tilde{\Lambda}x^{-7/4} \times \left(-\frac{27}{16}x^5\right)\frac{1+\frac{449}{108}x+\frac{22672}{9}x^{2.89}}{1+dx^4}$$

consistent with the PNTidal at the low frequency limit.

Pade approximation

Tidal phasing
different PN orders in PNTidal and NR calibrated models

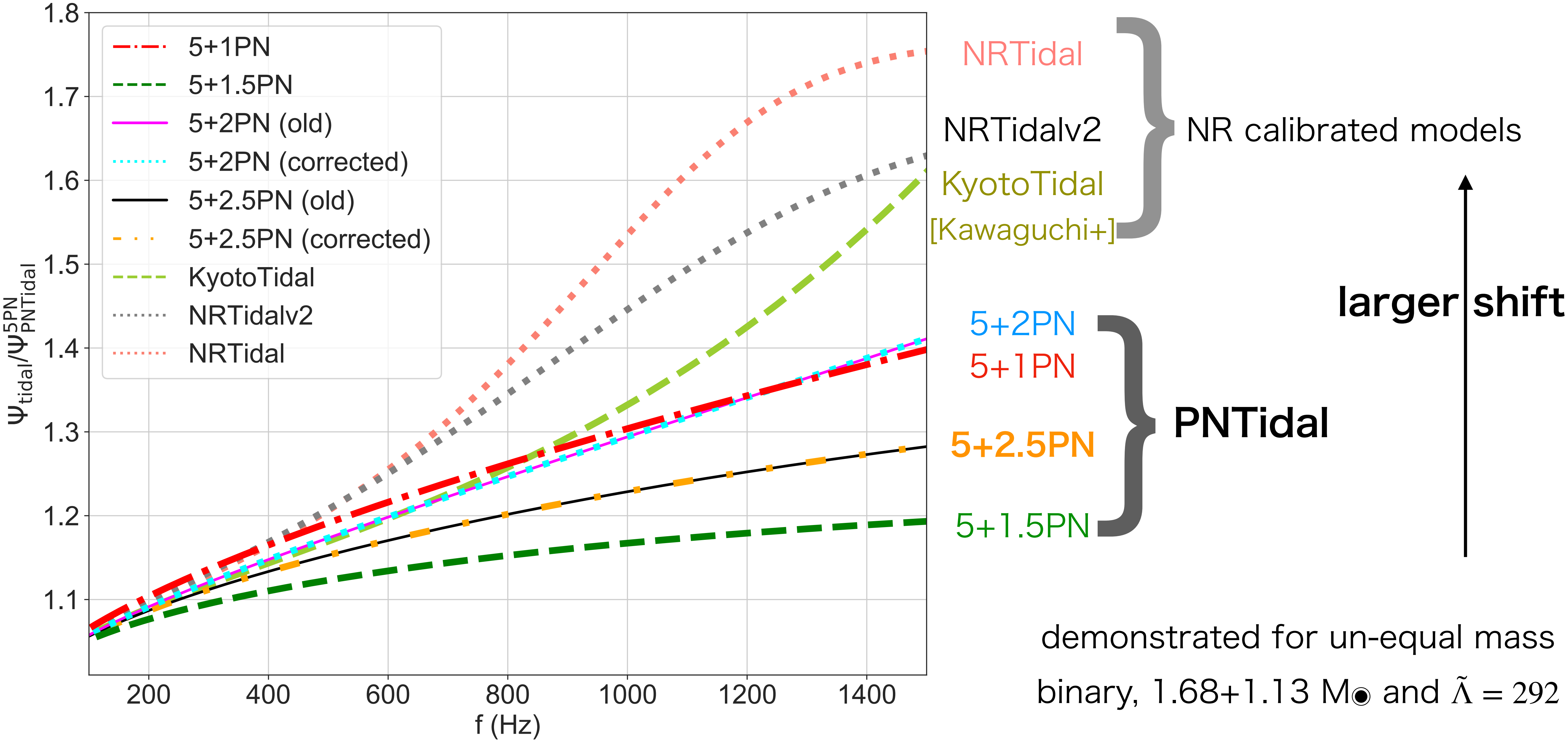

demonstrated for un-equal mass binary, 1.68+1.13 M⊙ and $\tilde{\Lambda} = 292$

NR calibrated models: **KyotoTidal**, **NRTidalv2**, and **NRTidal** give larger phase shift (more attractive) than **PNTidal.**

The terms at 5+1PN and 5+2PN give closer to NR calibrated models than the half-PN orders at 5+1.5PN and 5+2.5PN due to being repulsive.

Our analysis setup - parameter estimation

- **Post-Newtonian (PN) inspiral waveform model:**
  BBH (PP+Spin) + Tidal

- Phase $\Psi(f) = \Psi_{\rm BBH} + \Psi_{\rm tidal}$

Adding higher-order PN terms prevent $\tilde{\Lambda}$ biasing

- Point-particle: **TF2** (up to 3.5PN), **TF2g** (up to 5.5PN), **TF2+** (up to 6PN)
- Spin (aligned-spin): SO:1.5-3.5 PN, SS:2-3 PN,
- **Tidal effects: 5-5+2.5PN.**

Spin terms at other PN orders help to break degeneracies, e.g., $q - \chi_{\rm eff}$

We have implemented the correct **PNTidal** model.

- Amplitude up to 3 PN for BBH (PP+spin), up to 5+1PN for Tidal

- Priors: **low-spin prior: $|\chi_{1z,2z}|<0.05$;** uniform in [0, 3000] on $\tilde{\Lambda}$
astrophysically motivated

- **$f_{\rm high}$=1000 Hz to restrict to the inspiral regime**

- Bayesian inference library: Nested sampling in LALSUITE (LALInferenceNest)

Bayesian parameter estimation of GWs

Why Bayesian statistics and stochastic sampling

- A lot of parameters
- Parameter estimation (PE)
- Model comparison

Assuming stationary and Gaussian noise

$$\mathcal{L}(d|\boldsymbol{\theta}) \propto \exp\left[-\left\langle d - h(\boldsymbol{\theta}) \,\middle|\, d - h(\boldsymbol{\theta})\right\rangle\right]$$

Bayes' theorem

Likelihood

Prior

Posterior

$$p(\boldsymbol{\theta}|d) = \frac{\mathcal{L}(d|\boldsymbol{\theta})\pi(\boldsymbol{\theta})}{Z}$$

Evidence for the model

$$Z = \int d\boldsymbol{\theta}\,\mathcal{L}(d|\boldsymbol{\theta})\pi(\boldsymbol{\theta})$$

{d}: data set, θ ={masses, spins, Λ,$\cdots$}: parameters

For model comparison between A and B,

Bayes factor: the ratio of evidences

$$\mathrm{BF}_{\mathrm{A/B}} = \frac{Z_{\mathrm{A}}}{Z_{\mathrm{B}}}$$

Results

Follow-up analyses of GW170817 and GW190425 with **PNTidal** with f_{high}=1000 Hz to restrict to the inspiral regime.
Waveform systematics & Waveform model comparison:
➊ Comparison among point-particle part,
➋ Comparison among different PN orders in PNTidal,
➌ Comparison between PNTidal and NR calibrated models, and
➍ Constraints on NS EOSs

As a sanity check

Comparison between analyses by using the old and corrected tidal phase models for GW170817

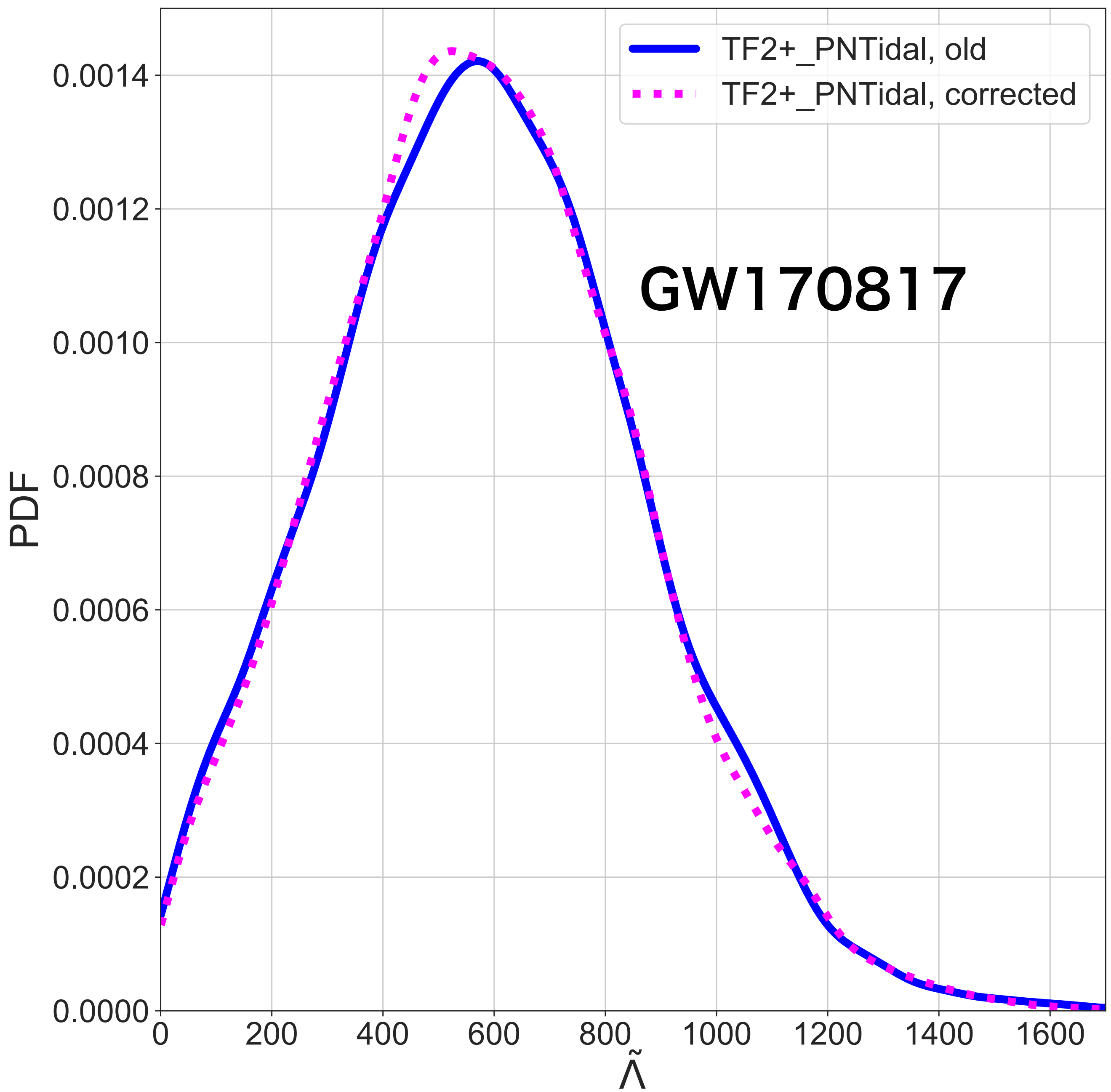

BBH baseline: **TF2+**,
low-spin prior, f_{high}=1000 Hz

No large difference between the estimates of $\tilde{\Lambda}$ by using **old** and **corrected** PNTidal phase models.

➊ Comparison among estimates of tidal deformability by using different point-particle baseline models

TF2 (up to 3.5PN), TF2g (up to 5.5PN), TF2+ (up to 6PN)

tidal part: **PNTidal**,
low-spin prior, f_{high}=1000 Hz

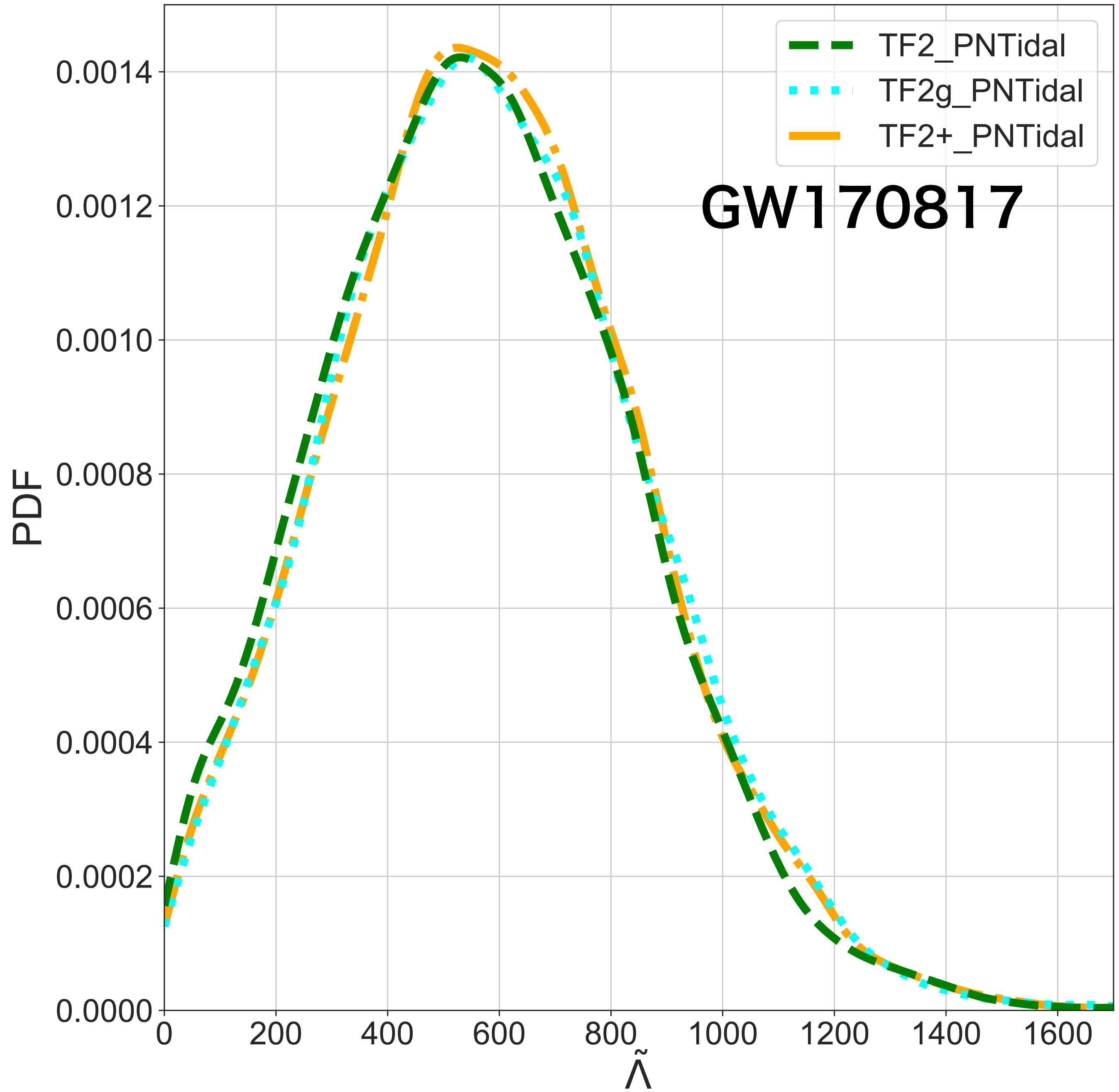

No large difference among the estimates of $\tilde{\Lambda}$ by using three point-particle baseline models: **TF2**, **TF2g**, and **TF2+**.

❷ Comparison among the estimates of tidal deformability $\tilde{\Lambda}$ with different PN orders in PNTidal

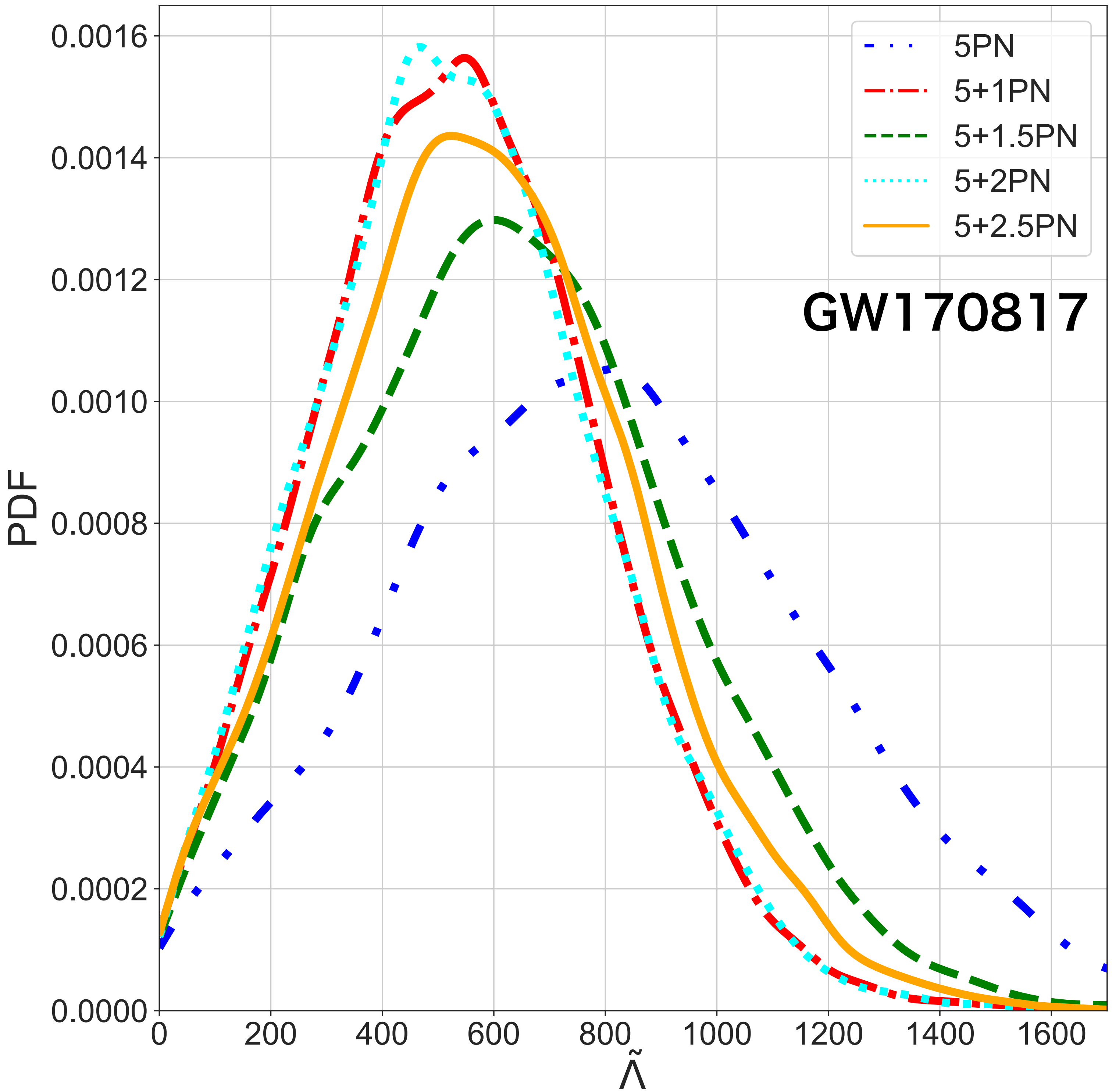

BBH baseline: **TF2+**,
low-spin prior, f_{high}=1000 Hz

An increase of PN order does not lead to a monotonic change in the estimates of $\tilde{\Lambda}$.

The terms up to 5+1PN and 5+2PN give smaller estimates on $\tilde{\Lambda}$. This is related to the half-PN orders at 5+1.5PN and **5+2.5PN** being repulsive.

Estimates of $\tilde{\Lambda}$ are consistent with the phase shift.

③ Comparison between estimates of $\tilde{\Lambda}$ for PNTidal and NR calibrated models

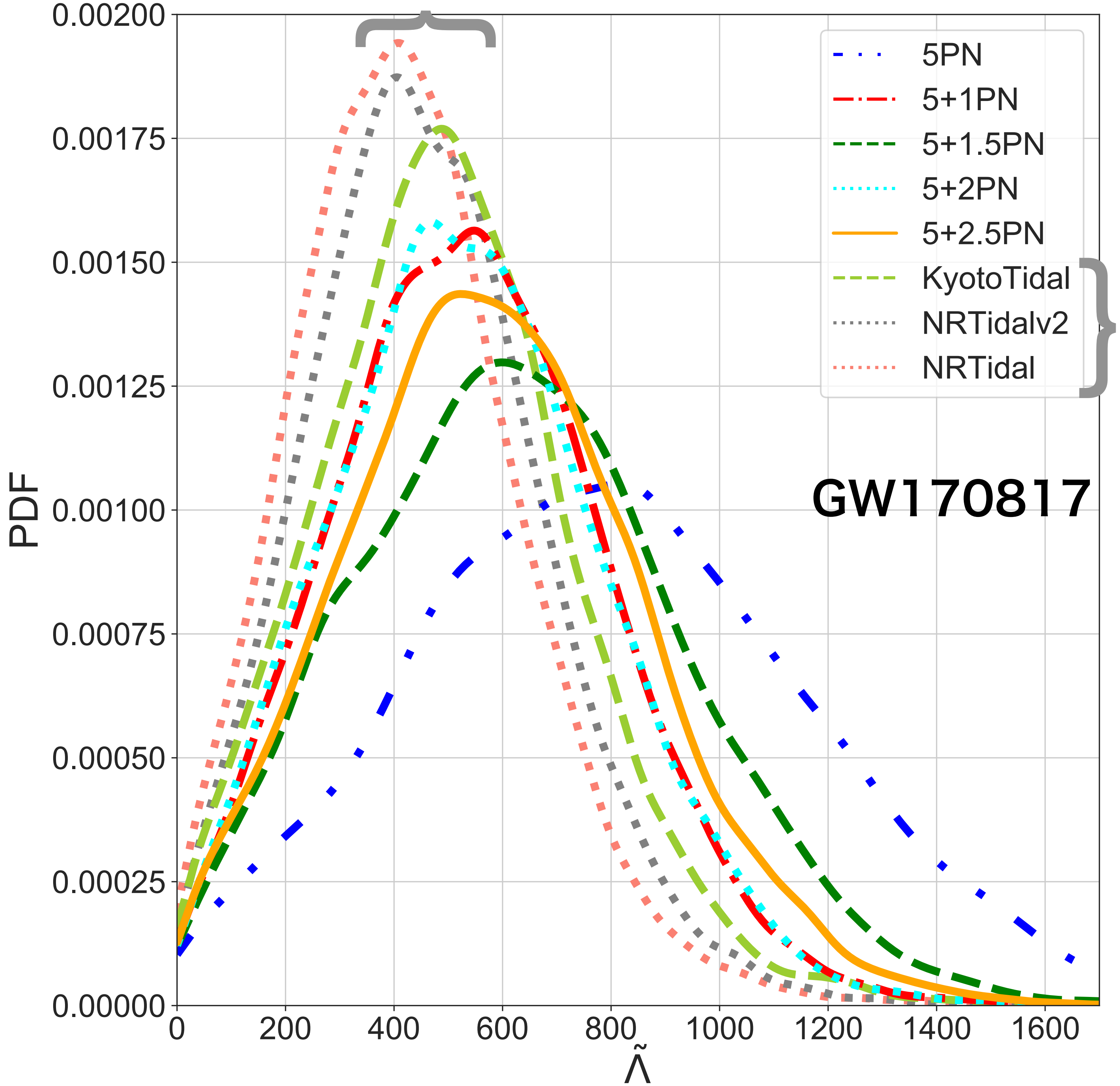

BBH baseline: **TF2+**,
low-spin prior, f_{high}=1000 Hz

NR calibrated models give smaller estimates of $\tilde{\Lambda}$ than PNTidal.

The terms up to 5+1PN and 5+2PN give closer estimates of $\tilde{\Lambda}$ with NR calibrated models, which is related to the half-PN orders at 5+1.5PN and **5+2.5PN** being repulsive.

Estimates of $\tilde{\Lambda}$ are consistent with the phase shift.

③ Waveform model comparison among PNTidal and NR calibrated models

BBH baseline: **TF2+**,
low-spin prior, f_{high}=1000 Hz

The log Bayes factor

$$\log \mathrm{BF}_{\mathrm{PNTidal/NR\ calibrated\ models}}$$

Waveform	GW170817
`KyotoTidal`	0.25
`NRTidalv2`	0.23
`NRTidal`	0.46
BBH (nontidal)	0.79

The log Bayes factors are less than 1, but positive values.

No preference among NR calibrated models over PNTidal.
However, **PNTidal** is mildly preferred compared to NR calibrated models.

This is consistent with [Gamba+, 2021].

❹ Constraints on EOSs for NSs with TF2+_PNTidal

low-spin prior, f_{high}=1000 Hz

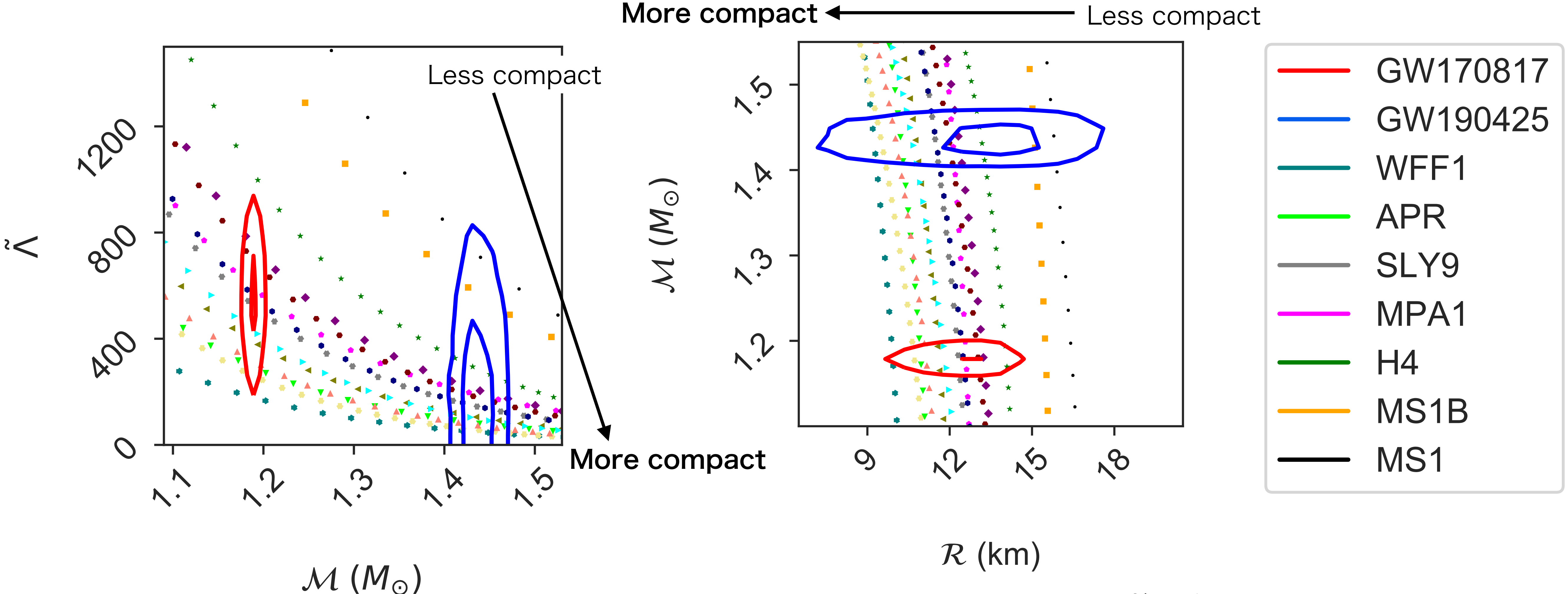

$$9\ \mathrm{km} \lesssim \mathscr{R} = 2\mathscr{M}\tilde{\Lambda}^{1/5} \lesssim 15\ \mathrm{km}$$

Less compact EOS models: MS1, MS1B, & H4 lie outside 90% credible regions for GW170817. → disfavored

Summary

Post-Newtonian (PN) approximation is theoretically rigid and can efficiently describe the inspiral regime.

Follow-up analyses of GW170817 and GW190425 with **PNTidal** focusing on the inspiral regime (f_{high}=1000 Hz).

Results

Waveform systematics & Waveform model comparison:

❶ Point-particle part: **No large difference among the estimates of $\tilde{\Lambda}$**

❷ Different PN orders in PNTidal: **An increase of PN order does not lead to a monotonic change in the estimates of $\tilde{\Lambda}$.**

❸ PNTidal vs NR calibrated models: **NR calibrated models give smaller $\tilde{\Lambda}$ than PNTidal. No preference among NR calibrated models over PNTidal. However, PNTidal is mildly preferred compared to NR calibrated models.**

❹ Constraints on NS EOSs: **GW170817 disfavor less compact models.**

Since KAGRA has recently joined the international GW network [O3GK 2020] and the Adv. LIGO and Adv. Virgo detectors are improving their sensitivities now, they will detect BNS signals with high SNR and provide more information on the sources in coming observation runs.

Other results

The 90% credible intervals of source parameters for GW170817 and GW190425 estimated using the **TF2+ PNTidal** model for f_{high} = 1000 Hz.

Parameters	GW170817	GW190425
Primary mass m_1	$1.36 - 1.57\ M_\odot$	$1.62 - 1.89\ M_\odot$
Secondary mass m_2	$1.19 - 1.37\ M_\odot$	$1.44 - 1.68\ M_\odot$
Chirp mass $\mathcal{M}$	$1.187^{+0.004}_{-0.002}\ M_\odot$	$1.436^{+0.022}_{-0.020}\ M_\odot$
Detector-frame chirp mass $\mathcal{M}^{\mathrm{det}}$	$1.1976^{+0.0001}_{-0.0001}\ M_\odot$	$1.4867^{+0.0003}_{-0.0003}\ M_\odot$
Mass ratio $q := m_2/m_1$	$0.76 - 1.00$	$0.76 - 1.00$
Total mass $M := m_1 + m_2$	$2.73^{+0.04}_{-0.01}\ M_\odot$	$3.31^{+0.06}_{-0.05}\ M_\odot$
Effective inspiral spin χ_{eff}	$0.003^{+0.014}_{-0.008}$	$0.009^{+0.015}_{-0.012}$
Luminosity distance D_{L}	$40.2^{+7.0}_{-14.0}$ Mpc	160^{+67}_{-73} Mpc
Binary tidal deformability $\tilde{\Lambda}$ (symmetric/HPD)	574^{+485}_{-425} / 574^{+433}_{-467}	295^{+578}_{-265} / 295^{+423}_{-295}

As a sanity check

Comparison between analyses by using the old and corrected tidal phase models for GW170817

BBH baseline: **TF2+**, low-spin prior, fhigh=1000 Hz, Tidal phase up to 7.5PN.

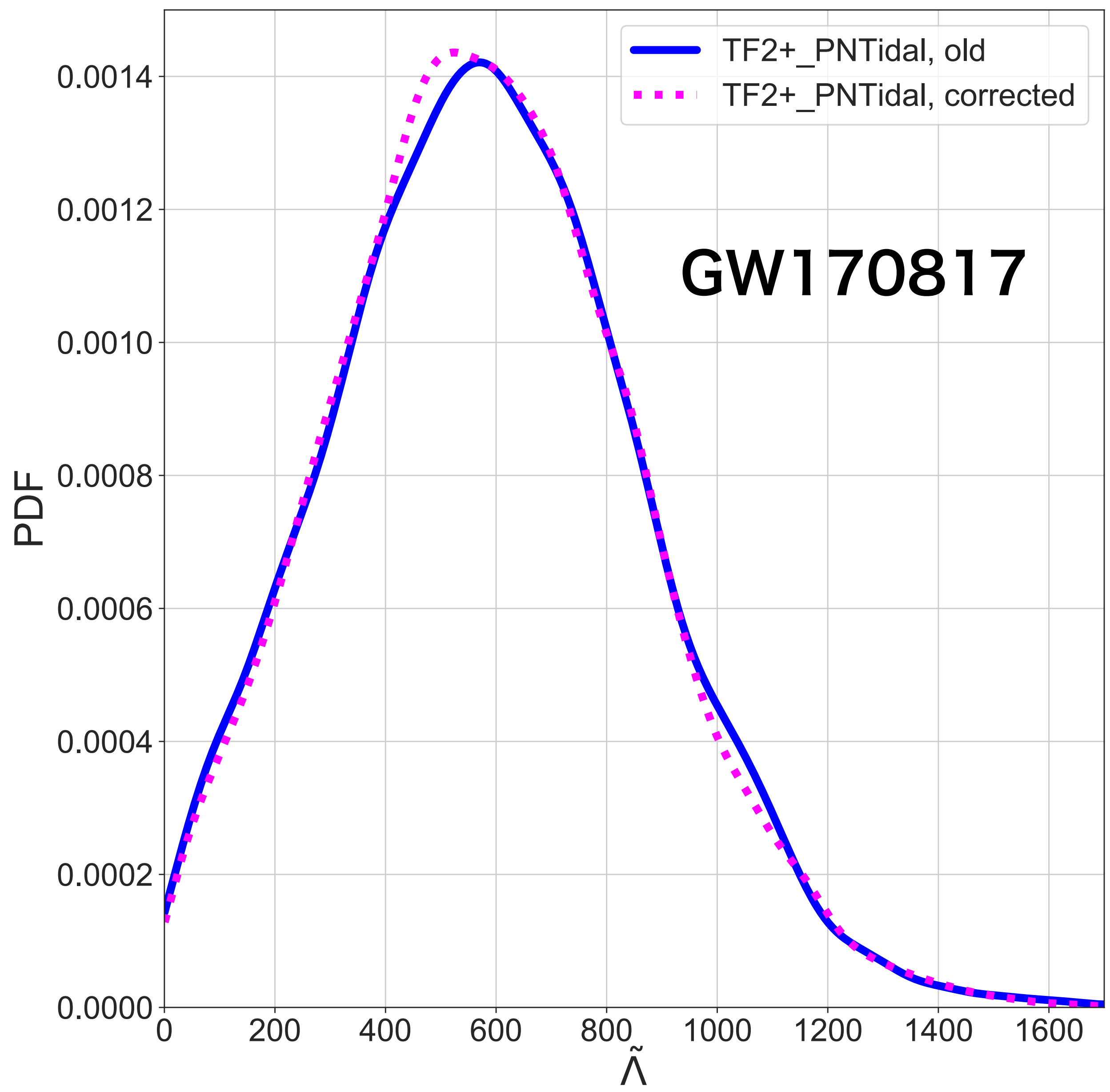

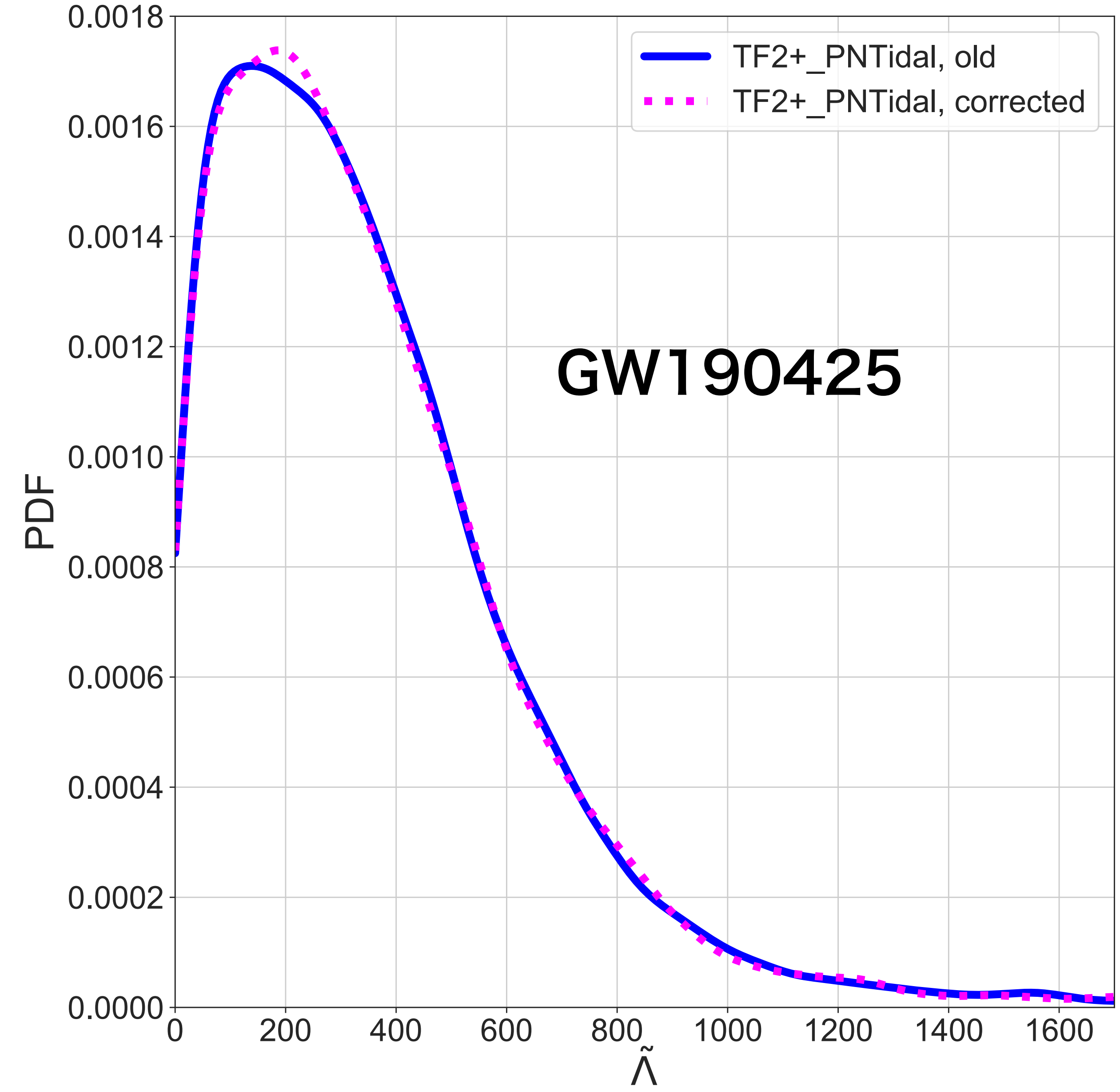

No large difference between the estimates of tidal deformability by using old and corrected tidal phase models

90% credible intervals of tidal deformability

	GW170817		GW190425	
	old	corrected	old	corrected
symmetric	579^{+486}_{-437}	574^{+485}_{-425}	297^{+589}_{-266}	295^{+578}_{-265}
HPD	579^{+441}_{-473}	574^{+433}_{-467}	297^{+424}_{-297}	295^{+423}_{-295}
$\log \mathrm{BF}_{\mathrm{corrected/old}}$	0.25		-0.15	

the median as a representative,
symmetric: median 5% - 95%,
hyghest-probability-density (HPD) interval

Comparison among estimates of the tidal deformability by using different point-particle baseline models

TF2 (up to 3.5PN), TF2g (up to 5.5PN), TF2+ (up to 6PN)

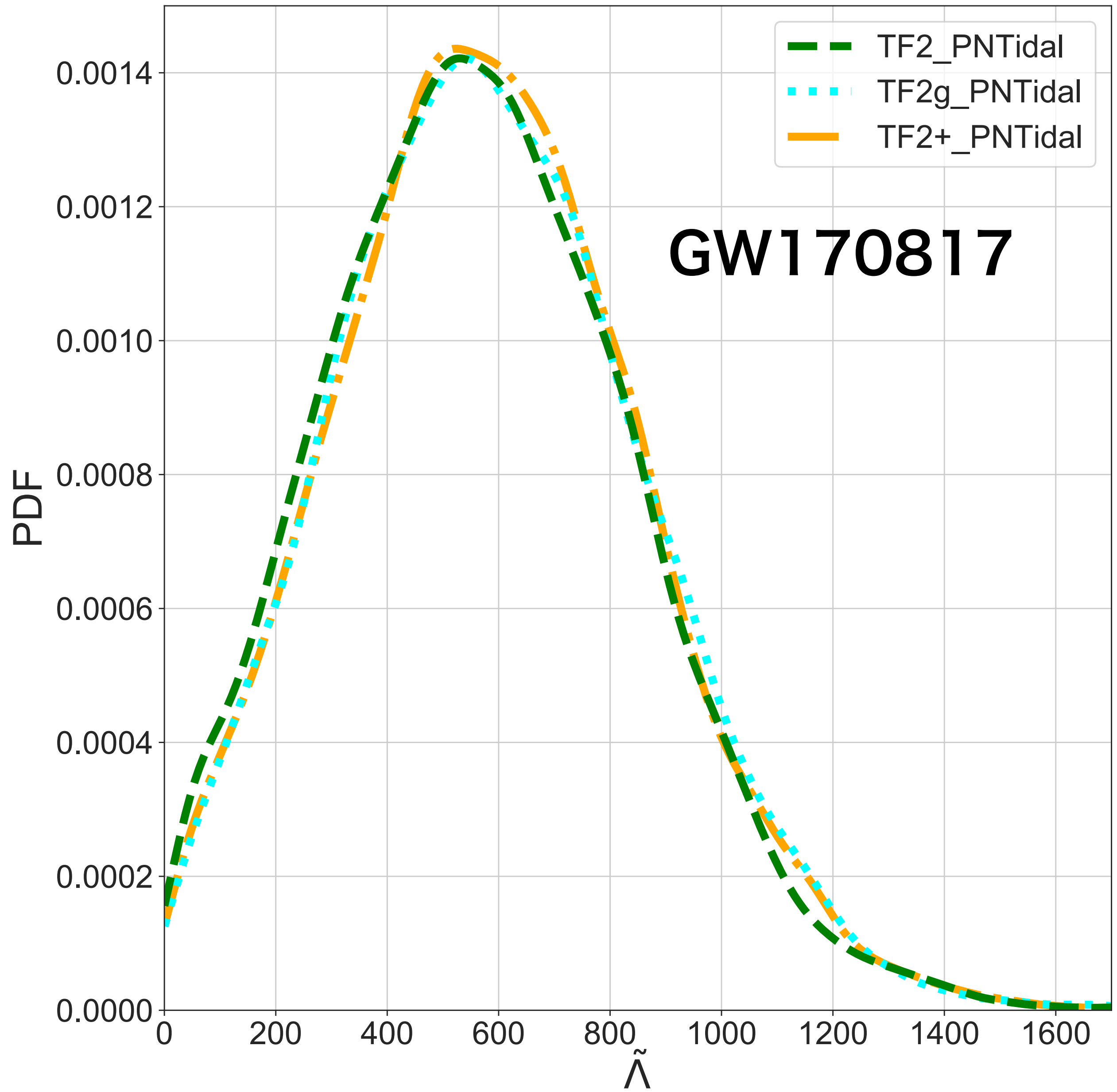

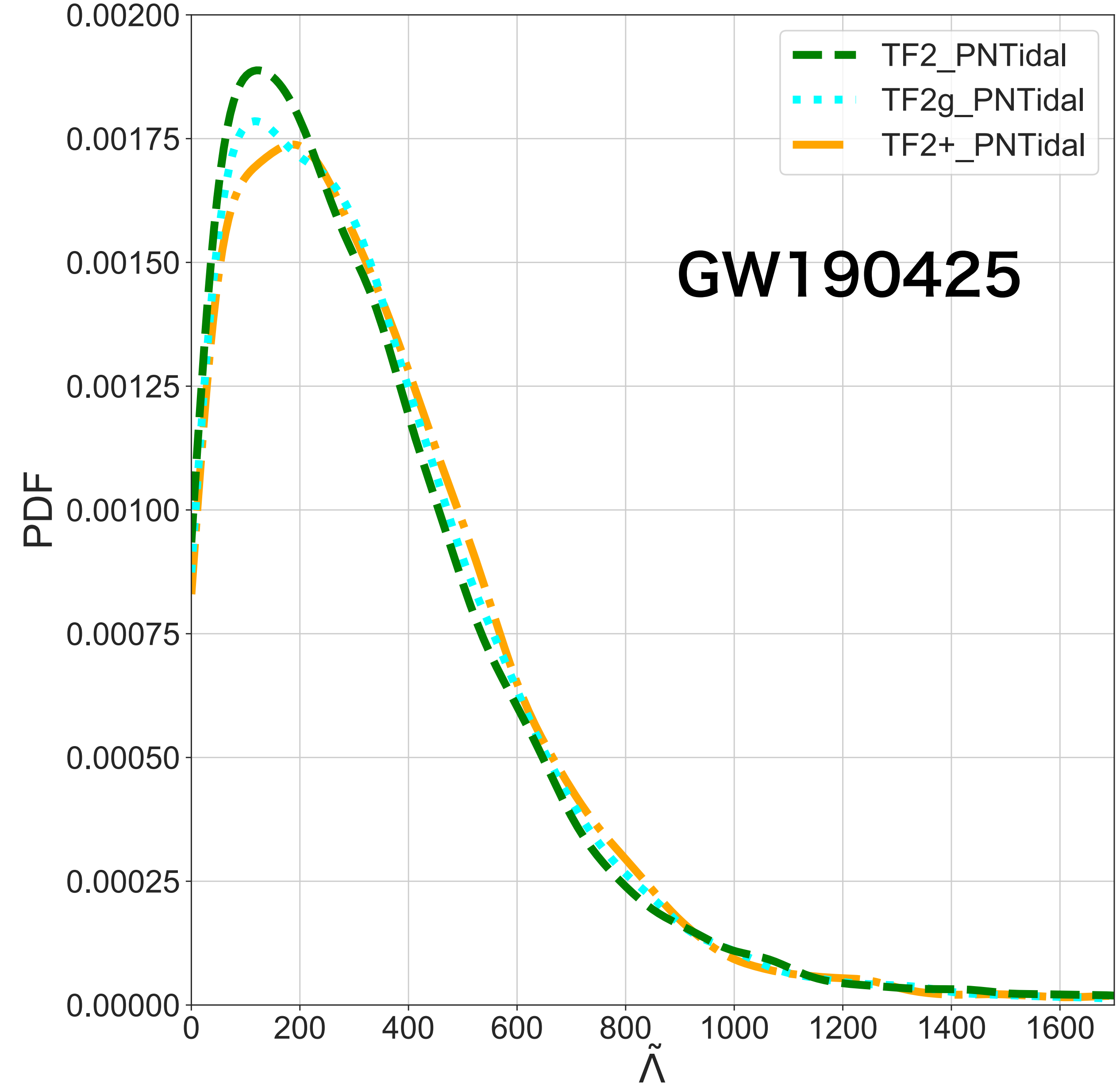

No large difference among the estimates of $\tilde{\Lambda}$ by using three point-particle baseline models, TF2, TF2g, and TF2+.

Comparison among the estimates of tidal deformability $\tilde{\Lambda}$ with different PN-orders in PNTidal

BBH baseline: **TF2+**, low-spin prior, f_{high}=1000 Hz

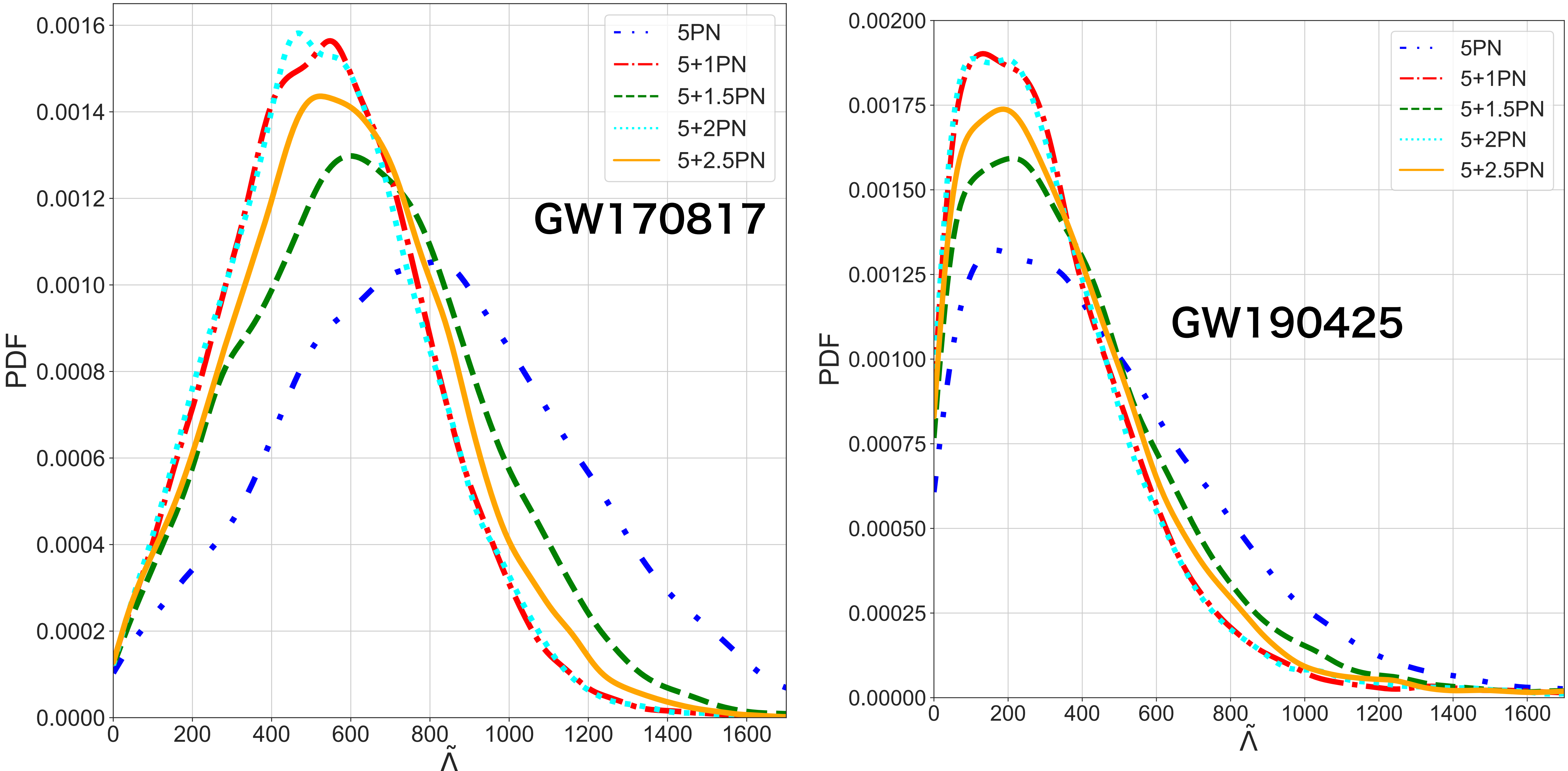

An increase of PN order does not lead to a monotonic change in the phase shift.

The terms up to 5+1PN and 5+2PN give tighter constraints on $\tilde{\Lambda}$. This is related to the half-PN orders at 5+1.5PN and 5+2.5PN being repulsive.

 Results are consistent with the phase shift.

Estimating the tidal deformability with the different PN-orders in the corrected PNTidal and NR calibrated models

BBH baseline: **TF2+**, low-spin prior, f_{high}=1000 Hz

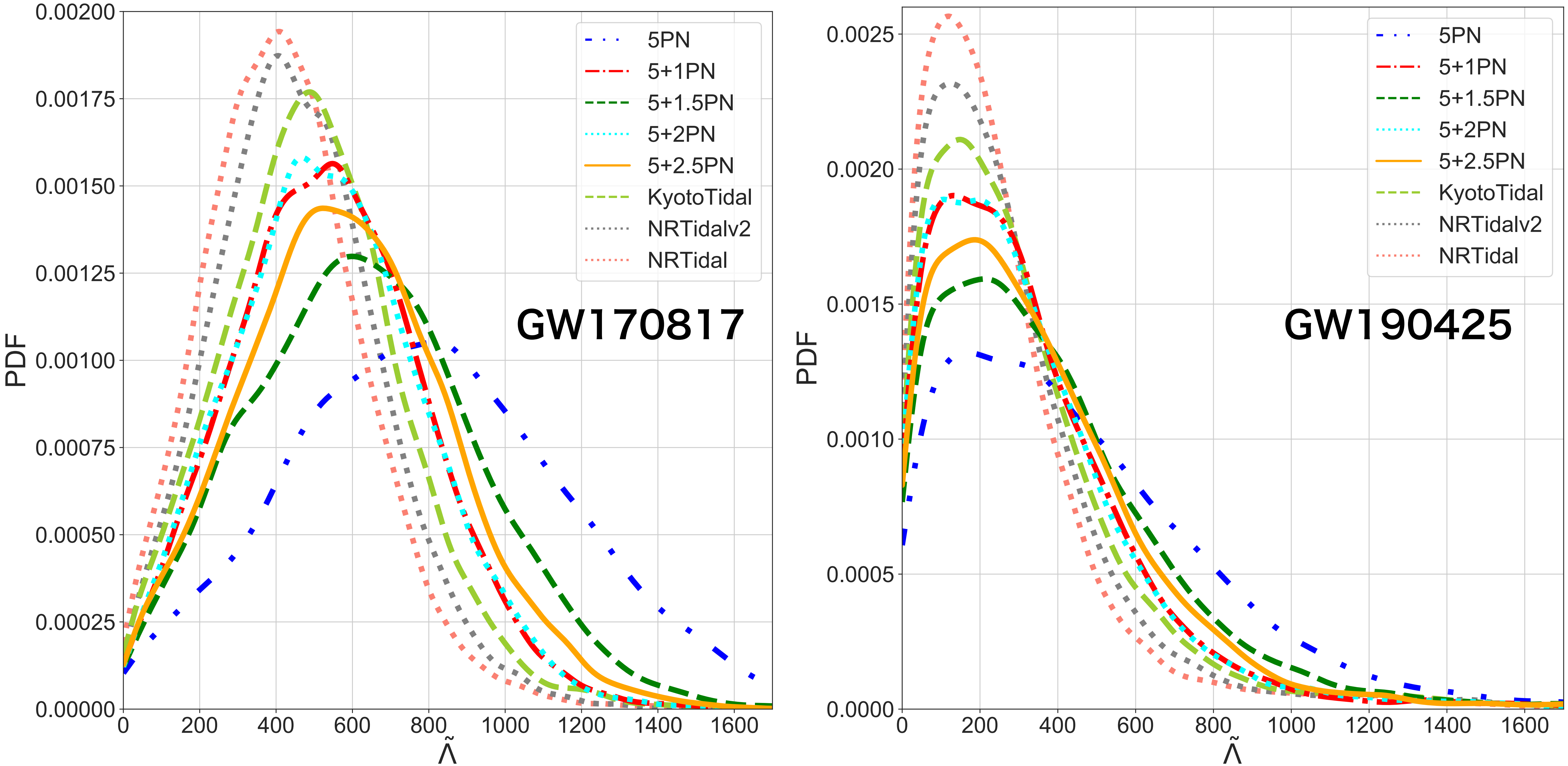

NR calibrated models give smaller estimates of $\tilde{\Lambda}$ than PNTidal.

The terms up to 5+1PN and 5+2PN give closer estimates of $\tilde{\Lambda}$ with NR calibrated models, which is related to the half-PN orders at 5+1.5PN and 5+2.5PN being repulsive.

 Results are consistent with the phase shift.

Waveform model comparison

TABLE III. The log Bayes factor of the TF2+_PNTidal model relative to the other point-particle baseline models, the TF2g_PNTidal and TF2_PNTidal models, $\log \mathrm{BF}_{\mathtt{TF2+\_PNTidal/TF2g\_PNTidal,\ TF2\_PNTidal}}$, for GW170817 and GW190425.

Waveform	GW170817	GW190425
TF2g_PNTidal	0.09	0.12
TF2_PNTidal	−0.20	−0.18

No preference among the different point-particle models

TABLE IV. The log Bayes factor of the terms at 5+2.5PN relative to the other PN orders, $\log \mathrm{BF}_{5+2.5\mathrm{PN/different\ PN}}$, for GW170817 and GW190425.

PN order	GW170817	GW190425
5PN	−0.17	−0.40
5+1PN	0.20	0.14
5+1.5PN	−0.04	−0.03
5+2PN	0.09	0.02

No preference among the PN orders

TABLE V. The log Bayes factor of PNTidal relative to the NR calibrated models: the KyotoTidal, NRTidalv2, and NRTidal models, $\log \mathrm{BF}_{\mathtt{PNTidal/NR\ calibrated\ model}}$, for GW170817 and GW190425. Only here, the $\tilde{\Lambda}$-form defined as Eq. (4) is used for the PNTidal model to take into account of the prior volume reduction. In the last row, we show the values for the TF2+ model as a BBH (nontidal) for comparison. The values indicate no preference model on GW170817.

Waveform	GW170817	GW190425
KyotoTidal	0.25	0.22
NRTidalv2	0.23	0.32
NRTidal	0.46	0.37
BBH (nontidal)	0.79	−1.58

No preference among NR calibrated models over PNTidal. However, PNTidal is mildly preferred compared to NR calibrated models.

Estimates for several binary parameters for GW170817

No large difference among the estimates of several binary parameters even for nontidal parameters by using three different point-particle baselines, TF2, TF2g, and TF2+, with PNTidal model.

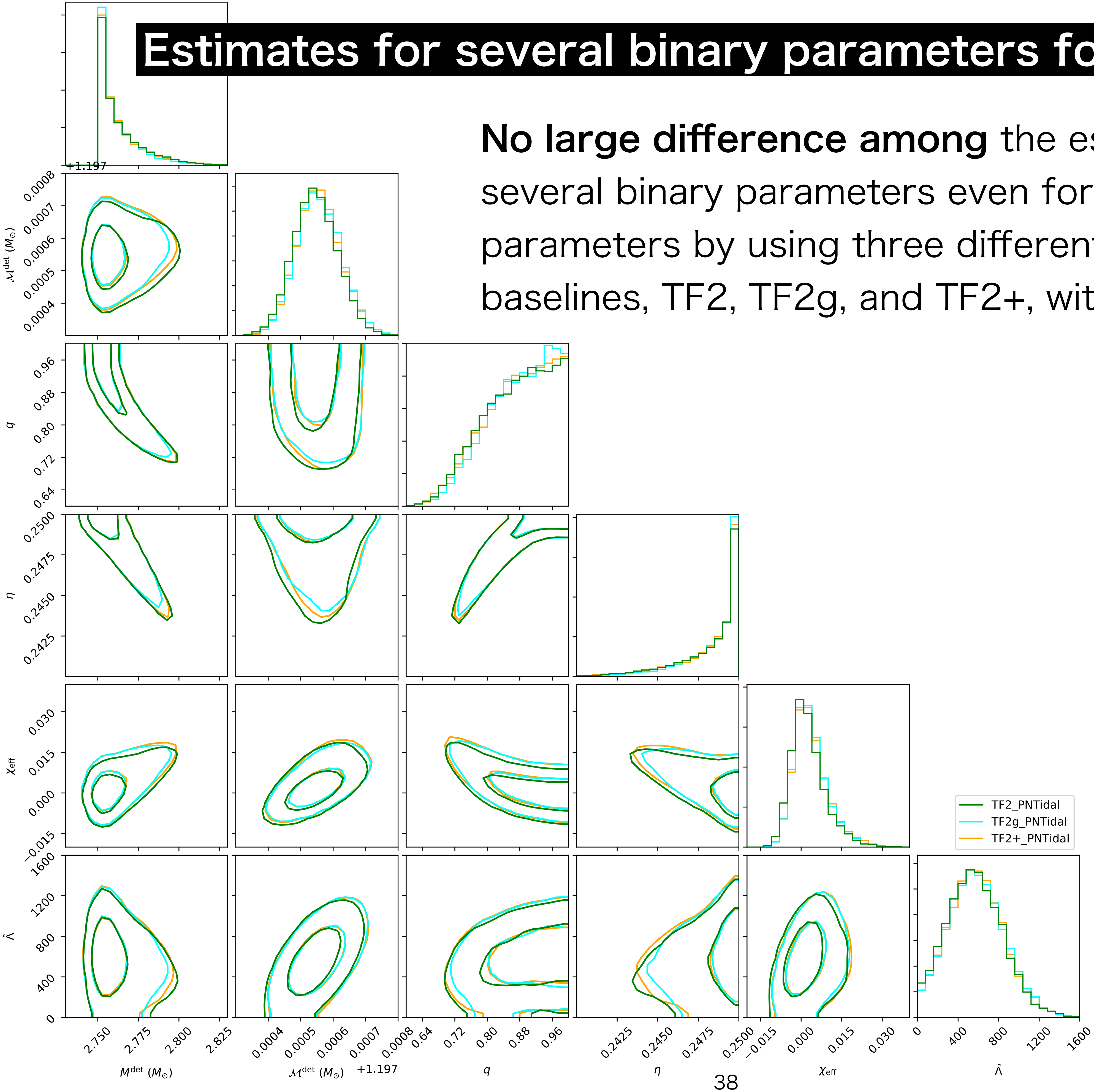

Estimates for several binary parameters for GW190425

No large difference among the estimates of several binary parameters even for nontidal parameters by using three different point-particle baselines, TF2, TF2g, and TF2+, with PNTidal model.